

Spectroscopic data of Rb-iso-electronic Zr and Nb ions for astrophysical applications

Jyoti,^a Mandeep Kaur,^a Bindiya Arora^{a*} and B. K. Sahoo^{b†}

^a*Department of Physics, Guru Nanak Dev University, Amritsar, Punjab-143005, India*

^b*Atomic, Molecular and Optical Physics Division, Physical Research Laboratory, Navrangpura, Ahmedabad-380009, India*

20 January 2022

ABSTRACT

We present high-accuracy spectroscopy data of line strengths, transition probabilities and oscillator strengths for the allowed transitions among the $nS_{1/2}$, $nP_{1/2,3/2}$ and $n'D_{3/2,5/2}$ states with $n = 5$ to 10 and $n' = 4$ to 10 of the Rb-iso-electronic Zr (Zr IV) and Nb (Nb V) ions. They can serve to analyse various astrophysical phenomena undergoing inside the heavenly bodies containing Zr and Nb elements. Since there is a lack of precise observational and calculated data for the spectroscopic properties in the above ions, their accurate determinations are of immense interest. The literature data, that are available only for a few selected low-lying transitions, have large discrepancies and they cannot be used reliably for the above purpose. After accounting for electron interactions through random phase approximation, Brückner orbitals, structural radiations and normalizations of wave functions in the relativistic many-body methods, we have evaluated the electric dipole amplitudes precisely. Combining these values with the observed wavelengths, the above transition properties and lifetimes of a number of excited states of the Zr IV and Nb V ions are determined and compared with the literature data.

Key words: Astronomical Data bases, Physical Data and Processes, Astronomical Data bases

1 INTRODUCTION

The emission spectra of heavenly bodies has been of great interest since last few decades so as to get the better insight of their atmosphere, chemical composition and evolution. A wide variety of analysis have been carried out globally to provide the data for abundance of various spectral lines in these bodies, however, many of them are still unknown. A diversity of elements and ions have been observed in these spectra out of which zirconium (Zr) and niobium (Nb) are of interest to us, as they play important roles in the decay processes (Nilsson et al. 2010; García-Hernández et al. 2007), which are generally the combination of slow (s) and rapid (r) neutron-capture nucleosynthesis processes and are specifically responsible for the detection of spectral lines of lighter elements. The presence of Nb and its ions has been observed in the atmosphere of three metal-poor stars HD 209621, HD 218732 and HD 232078, the standard star Arcturus (Zács et al. 2011), Sun and AGB M and MS stars (Nilsson et al. 2010; Palme et al. 2014). The radionuclide of ^{92}Nb decays to ^{92}Zr by neutron-capture process with a half-life of 37 Ma (Holden 1989). The presence of live ^{92}Nb in early Solar System was first obtained from the iron meteorite Toluca (Harper Jr 1996), which further offered a unique opportunity to estimate the timescale of the early Solar System (Iizuka et al. 2016). Heavy element stars such as ROA

371, ROA 5293, and ROA 3812 in the globular cluster Omega Centauri consist of a considerable abundance of s-process elements; i.e. Rb, Y and Zr (Vanture et al. 1994). Besides, the presence of Zr IV lines has been detected in the University College London Echelle Spectrograph (UCLES) of a He-rich hot sdB star, LS IV-14°116 on the Anglo-Australian Telescope (AAT) (Jeffery et al. 2011), in the Far Ultraviolet Spectroscopic Explorer (FUSE) spectra of hot subdwarf B stars (sdB) (Chayer et al. 2006) and in the UV spectra of hot white dwarfs, G191–B2B and RE0503–289 (Rauch et al. 2017). The spectral properties obtained from measurements and calculations are the prerequisites of stellar-atmosphere modeling (Rauch et al. 2016).

The stellar-modeling aspires the determination of chemical abundances and energy transport through a star, which requires the knowledge of reliable values of oscillator strengths as well as transition probabilities (Martin et al. 1992) of the emission spectra from the elements present in the stars. Accurate values of absorption oscillator strengths as well as transition probabilities are needed for correctly modeling and analysing the stellar intensities of the lines so as to infer fundamental stellar parameters (Ruffoni et al. 2014) such as mass M , radius R and luminosity L of any star (Wittkowski 2005). The information regarding the oscillator strengths and transition probabilities are also useful in the analysis of interstellar and quasar absorption of lines as well as the photospheric abundance of the considered element in a star (Rauch et al. 2017), the construction of kinetic models of plasma processes and for the investigation of

* bindiya.phy@gndu.ac.in

† bijaya@prl.res.in

processes in thermonuclear reactor plasma (Glushkov et al. 1996; Tayal 2012). They are also needed for the estimation of the electron collisional rate coefficients and photoionization cross-sections so as to explain various scattering phenomena (Griem & (Firm) 1974; Zeppen 1995; Orban et al. 2006). The precise evaluation of line strengths is also useful for the assessment of the Stark Broadenings of spectral lines, which is pivotal for the analysis of astrophysical phenomena (Alonso-Medina & Colón 2014). Due to this fact, the determination of radiative properties of lines present in the emission spectra of stars has become of sheer importance in the astrophysical studies.

To our knowledge, precise observational data of the spectroscopic properties of Rb-isoelectronic Zr (Zr IV) and Nb (Nb V) ions are not available in the literature. Limited theoretical results have been reported on the properties of these ions, but they are only for a few low-lying transitions. The data for transition probabilities, oscillator strengths, lifetimes, and branching ratios for Zr IV and Nb V were first provided by Lindgard and Nielsen in 1977 by using numerical Coulomb approximation (Lindgård & Nielsen 1977). Later on, in 1979, Migdalek and Baylis studied oscillator strengths for the lowest $5S_{1/2} \rightarrow 5P_{1/2,3/2}$ transitions for Rb-isoelectronic series, which included the data for Zr IV and Nb V, using relativistic single-configuration Hartree-Fock method and investigated the roles of core polarisation effects for their accurate determination (Migdalek & Baylis 1979). Karwowski and Szulkin, in 1981, evaluated the ground state energies and also determined the oscillator strengths for the $5S \rightarrow 5P$ transitions of Zr IV using the modified relativistic Hartree-Fock method (Karwowski & Szulkin 1981). Sen and Puri had calculated dipole oscillator strengths for these transitions in 1989 using the Local Spin Density approximation and compared them with the then available experimental and theoretical data (Sen & Puri 1989). A few years later, in 1996, Glushkov et al. determined oscillator strengths for the $5S \rightarrow 5P$, $5P \rightarrow nD$ ($n=4,5$) and $4P \rightarrow 4F$ transitions of Nb V ion using a non-relativistic method with the Coulomb screened potential approximation (Glushkov et al. 1996). Zilitis had also evaluated transition probabilities of the $5S_{1/2}-5P_{1/2,3/2}$, $4D_{3/2}-5P_{1/2,3/2}$, and $4D_{3/2}-4F_{5/2}$ transitions as well as the lifetimes of the $5P_{1/2}$ and $5P_{3/2}$ states of both the Zr IV and Nb V ions using the Dirac-Fock (DF) method in 2007 (Zilitis 2007) and later, in 2009, he extended the calculations for the oscillator strengths of the $4D_{3/2}-nP_{1/2,3/2}$ and $4D_{3/2}-nF_{5/2}$ transitions of both the ions (Zilitis 2009). In 2016, transition energies for the $5S-5P$, $5P-4D$, $4D-4F$ and $5D-4F$ transitions of these ions were evaluated by Migdalek on the basis of model potential in the DF method (Migdalek 2016). Das et.al. studied spectroscopic properties of a few Rb-like ions including Zr IV and Nb V ions using the relativistic coupled-cluster method in 2017 (Das et al. 2017). They calculated the matrix elements due to electric and magnetic multipole operators, lifetimes and oscillator strengths for different transitions and studied correlation behaviors in the Rb-isoelectronic series from Y III through Tc VII ions.

On account of evidence of presence of Zr and Nb in astrophysical bodies, it is necessary to seek through the radiative data of as many as spectral lines. As mentioned above, these data are mainly available on the $ns^2S_{1/2} \rightarrow np^2P_{1/2,3/2}$, $n = 4, 5$, $5p^2P \rightarrow nd^2D$, ($n = 4, 5$), $4p^2P \rightarrow 4f^2F$, $4D_{3/2}-$

$nP_{1/2,3/2}$ and $4D_{3/2}-nF_{5/2}$ transitions only in the above ions. In this work, we extend the calculations on the spectroscopic data for a large number of transitions including high-lying lines. In particular, we have determined the allowed electric dipole (E1) matrix elements for the transitions among the $nS_{1/2}$, $nP_{1/2,3/2}$, and $n'D_{3/2,5/2}$ states with $n = 5$ to 10 and $n' = 4$ to 10 of the Zr IV and Nb V ions except for a few transitions which were not gauge invariant. Combining these data with the observed transition wavelengths, we have estimated the oscillator strengths, transition probabilities and radiative lifetimes of a number of excited states precisely. Moreover, we have calculated energies of a few low-lying and excited states for both the ions and compared them with the values listed in the National Institute of Science and Technology atomic database (NIST AD) (Ralchenko et al. 2008). The aforementioned data can be immensely useful for analysing astrophysical processes; especially in the metal-poor stars HD 209621, HD 218732 and HD 232078, Arcturus and white dwarfs.

The paper is organized as follows: In Sec. 2, we provide the theoretical formulae for the E1 matrix elements, transition probabilities, oscillator strengths and lifetime of the atomic states. Sec. 3 discusses all the acquired data from present work and compares with the previously reported values, while findings are concluded in Sec. 4. All the results are given in atomic units (a.u.) unless stated otherwise.

2 THEORETICAL ASPECTS

2.1 Formulae for spectroscopic quantities

Transitions among the atomic states are dominantly driven by the E1 channel when allowed. Here, we analyze the transition properties only due to the E1 channel as electrons can decay from the excited states of the ions of our interest mainly through this channel. The transition probability due to the E1 channel (A_{vk}^{E1}) from an upper level $|\Psi(v)\rangle$ to a lower level $|\Psi(k)\rangle$ with the corresponding angular momentum J_v and J_k respectively is given (in s^{-1}) by (Kelleher & Podobedova 2008)

$$A_{vk}^{E1} = \frac{2}{3} \alpha c \pi \sigma \left(\frac{\alpha \sigma}{R_\infty} \right)^2 \frac{S^{E1}}{g_v}, \quad (1)$$

where $R_\infty = \frac{\alpha^2 m_e c}{2h}$ is the Rydberg constant with the Planck's constant h and mass of electron m_e , α is fine structure constant $\alpha = \frac{e^2}{4\pi\epsilon_0\hbar c}$, c is the speed of light, $\sigma = E_v - E_k$ is the excitation energy of the transition, S^{E1} is the line strength and $g_v = 2J_v + 1$. Here, $S^{E1} = |\langle J_v || \mathbf{D} || J_k \rangle|^2$ (Nahar 1995) with the E1 operator $\mathbf{D} = \sum_j \mathbf{d}_j = -e \sum_j \mathbf{r}_j$ for the j^{th} electron being at position \mathbf{r}_j . On substituting the values of fundamental constants as $\alpha = 7.297352 \times 10^{-3}$, $R_\infty = 1.0973731 \times 10^5 \text{ cm}^{-1}$ and $c = 29979245800 \text{ cm s}^{-1}$ (Mohr et al. 2016), the above formula yields (Kelleher & Podobedova 2008)

$$A_{vk}^{E1} = \frac{2.0261269 \times 10^{18}}{\lambda^3 g_v} S^{E1}, \quad (2)$$

where λ is the wavelength of transition in Å.

The absorption oscillator strengths of the allowed transitions (f_{kv}^{E1}) are very useful in the astrophysical analyses, which can be determined from the lower $|\Psi(k)\rangle$ level to the upper $|\Psi(v)\rangle$ level using its transition probability which

follows as (Kelleher & Podobedova 2008; Sobelman 1979; Kaur et al. 2020)

$$\begin{aligned} f_{kv}^{E1} &= \left(\frac{R_\infty}{2c\alpha^3\pi} \right) \frac{g_v}{g_k} \times \frac{A_{vk}^{E1}}{\sigma^2} \\ &= \frac{1}{3\alpha} \left(\frac{\alpha\sigma}{R_\infty} \right) \times \frac{S^{E1}}{g_k} \\ &= \frac{303.756}{g_k\lambda} \times S^{E1}. \end{aligned} \quad (3)$$

The radiative lifetime (τ) of the excited state $|\Psi(v)\rangle$ can also be obtained by taking reciprocal of the total transition probabilities of all the lower possible transitions from that level (Qin et al. 2019; Kaur et al. 2020); i.e.

$$\tau_v = \frac{1}{\sum_k A_{vk}}, \quad (4)$$

where sum over k denotes all possible states ($|\Psi(k)\rangle$) to which allowed transitions from $|\Psi(v)\rangle$ are possible.

2.2 Methods for calculations

The presence of the two-body electromagnetic interactions among the electrons within an atomic system poses challenge to solve atomic wave functions accurately. In a typical approach, atomic wave functions are obtained by calculating them using a mean-field approach then incorporating the electron correlation effects due to the neglected interactions systematically. These correlation effects are classified into various physical effects such as core-polarization and pair-correlation effects, which behave differently for accurate description of wave functions depending upon the electronic configurations of atomic systems. Large differences among the previous calculations of transition properties in the considered ions using a variety of many-body methods (Lindgård & Nielsen 1977; Migdalek & Baylis 1979; Karwowski & Szulkin 1981; Glushkov et al. 1996; Zilitis 2007; Das et al. 2017) suggest that the roles of the electron correlation effects are significant and they should be accounted for meticulously in order to obtain reliable results. In view of this, we include the electron correlations due to the core-polarization effects through random-phase approximation (RPA), pair-correlation effects through the Brückner orbitals (BOs) and their couplings through the structural radiations (SRs) in the determination of atomic wave functions. Corrections in the results due to normalization of the wave functions (Norms) are also estimated explicitly. A brief description of the procedures adopted to incorporate the above physical effects in the calculations is given below.

We first evaluate the mean-field wave function ($|\Phi_0\rangle$) of the $[4p^6]$ configuration of the considered ions using the DF method in which the atomic Hamiltonian is expressed as $H = H_0 + V_I$ with the DF Hamiltonian H_0 and residual interaction V_I , given in atomic units (a.u.) by

$$H_0 = \sum_i \epsilon_i a_i^\dagger a_i \quad (5)$$

and

$$V_I = \frac{1}{2} \sum_{ijkl} g_{ijkl} a_i^\dagger a_j^\dagger a_l a_k - \sum_{ij} u_{ij}^{DF} a_i^\dagger a_j, \quad (6)$$

where the sums over i, j, k and l include all electron orbitals, ϵ_i are the eigenvalues of the one-electron DF orbitals,

g_{ijkl} is the two-body matrix element of the Coulomb interaction ($\frac{1}{r_{ij}}$) and u_{ij}^{DF} is the DF potential (Blundell et al. 1987; Johnson et al. 1996; Safronova et al. 2005). The working DF wave functions ($|\Phi_v\rangle$) of the interested states of both Zr IV and Nb V are obtained by appending the respective valence orbital v to $|\Phi_0\rangle$ for the configurations $[4p^6]v$; i.e. $|\Phi_v\rangle = a_v^\dagger |\Phi_0\rangle$. The choice this V^{N-1} DF potential with (N number of electrons of the system) is to facilitate for calculating as many as states having common closed core $[4p^6]$. The neglected core-valence effects at this level are included as corrections in the next level.

The corrections over the DF wave functions due to the electron correlation effects are estimated using the perturbative analysis of V_I by expressing the exact wave function of the state ($|\Psi_v\rangle$) in the relativistic many-body perturbation theory (RMBPT) analysis as

$$|\Psi_v\rangle = |\Phi_v\rangle + |\Phi_v^{(1)}\rangle + |\Phi_v^{(2)}\rangle + \dots \quad (7)$$

and its energy (E_v) as

$$E_v = E_v^{(0)} + E_v^{(1)} + E_v^{(2)} + \dots, \quad (8)$$

where superscripts $k = 1, 2$ etc. denote order of perturbation and the zeroth-order energy is $E_v^{(0)} = \sum_k \epsilon_k$. After obtaining the wave functions, the E1 matrix element between the states $|\Psi_v\rangle$ and $|\Psi_w\rangle$ is calculated as

$$D_{wv} = \frac{\langle \Psi_w | D | \Psi_v \rangle}{\sqrt{\langle \Psi_w | \Psi_w \rangle \langle \Psi_v | \Psi_v \rangle}}. \quad (9)$$

As mentioned above contributions from the perturbative corrections are categorized into RPA, BO, SR and Norm contributions by expressing (Blundell et al. 1987; Johnson et al. 1996)

$$D_{wv} = D_{wv}^{DF} + D_{wv}^{RPA} + D_{wv}^{BO} + D_{wv}^{SR} + D_{wv}^{Norm}, \quad (10)$$

where $D_{wv}^{DF} \equiv d_{wv} = \langle \phi_w | d | \phi_v \rangle$ with the DF single particle wave functions $|\phi_v\rangle$ and $|\phi_w\rangle$. Since core-polarization effects contribute significantly, they are included through RPA self-consistently to all-orders by defining (Johnson 2007; Johnson et al. 1996):

$$D_{wv}^{RPA} = \sum_{\zeta=1}^{\infty} \sum_{na} \left[\frac{d_{an}^{(\zeta)} \tilde{g}_{wnva}}{\epsilon_v + \epsilon_a - \epsilon_n - \epsilon_w} + \frac{\tilde{g}_{wavn} d_{na}^{(\zeta)}}{\epsilon_w + \epsilon_a - \epsilon_n - \epsilon_v} \right] \quad (11)$$

for $\tilde{g}_{ijkl} = g_{ijkl} - g_{ijlk}$ and superscript ζ represents iteration number with

$$d_{an}^{(\zeta)} = d_{an} + \sum_{bm} \left[\frac{d_{bm}^{(\zeta-1)} \tilde{g}_{amnb}}{\epsilon_v + \epsilon_b - \epsilon_m - \epsilon_w} + \frac{\tilde{g}_{abnm} d_{mb}^{(\zeta-1)}}{\epsilon_w + \epsilon_b - \epsilon_m - \epsilon_v} \right],$$

and

$$d_{na}^{(\zeta)} = d_{na} + \sum_{bm} \left[\frac{d_{bm}^{(\zeta-1)} \tilde{g}_{namb}}{\epsilon_v + \epsilon_b - \epsilon_m - \epsilon_w} + \frac{\tilde{g}_{nbam} d_{mb}^{(\zeta-1)}}{\epsilon_w + \epsilon_b - \epsilon_m - \epsilon_v} \right].$$

The initial values correspond to $d_{an}^{(0)} = 0$ and $d_{an}^{(1)} = d_{an}$. The a, b, \dots, m, n, \dots and w, v indices in the subscripts denote for the occupied, virtual and valence orbitals, respectively.

The leading-order electron correlation contributions through BO and SR arise at the third-order perturbation level. We include these contributions using the procedure followed by Johnson et al. in (Johnson et al. 1996) in the present calculations. The Norm contributions have been estimated

Table 1. Our calculated energy values (cm^{-1}) for few low lying and excited states using RMBPT method for Zr IV and Nb V along with their comparison with experimental energies provided in NIST AD (Ralchenko et al. 2008). Ground state is taken at 0 cm^{-1} .

State	Zr IV		Nb V	
	Energy (cm^{-1})	NIST (cm^{-1})	Energy (cm^{-1})	NIST (cm^{-1})
$4D_{5/2}$	1109.05	1250.70	1741.83	1867.40
$5S_{1/2}$	34572.42	38258.35	72113.24	75929.60
$5P_{1/2}$	76313.25	81976.50	123581.01	129195.20
$5P_{3/2}$	78607.03	84461.35	126972.64	132800.00
$5D_{3/2}$	138820.28	146652.40	203904.11	211694.00
$5D_{5/2}$	139158.53	147002.46	204434.63	212238.40
$6S_{1/2}$	143994.52	152513.00	219451.86	228496.30
$6P_{1/2}$	160898.86	169809.71	241153.11	250506.50
$6P_{3/2}$	161848.63	170815.11	242602.26	252023.3
$6D_{3/2}$	188289.90	197765.10	277261.63	287163.60
$6D_{5/2}$	188450.91	197930.43	277515.77	287425.60
$7S_{1/2}$	190309.74	200123.69	284180.44	294736.00
$7P_{1/2}$	198869.74	208783.36	295423.65	305986.50
$7P_{3/2}$	199358.47	209297.66	296185.80	306788.10
$7D_{3/2}$	213460.26		314942.71	325705.70
$7D_{5/2}$	213550.09		315085.29	325854.80
$8S_{1/2}$	214494.56	224813.48	318702.16	329884.20

by adopting the approach discussed in (Blundell et al. 1987) and approximating the atomic wave function at the second-order perturbation theory.

It is obvious from the above discussion that our procedure incorporates various physical effects due to the electron correlation effects that are complete through the third-order perturbation and core-polarization effects to all-orders. To verify reliability in the calculations of the E1 matrix elements and estimate their uncertainties, we use both the length (L) and velocity gauge (V) expressions in the relativistic form (e.g. see (Kaur et al. 2020)). The differences in the results from both the gauge forms can be safely used as the maximum uncertainties associated with our calculated E1 matrix elements. Since calculations with length gauge expression converge faster with respect to the number of configurations, we believe that results from the length gauge expression are more reliable. Thus, we consider these results as the central values. In a few transitions, it is noticed that the length gauge and velocity gauge results differ by more than 50%. In such cases, it is possible to improve calculations by considering higher-order contributions through BO and SR effects, but they are computationally more expensive. Therefore, we do not endorse the results obtained using above method for such few cases and do not present them in this work.

Table 2: The line strengths (S_{vk}) (in a.u.) from both the L and V gauge expressions, wavelengths (λ) (in Å), transition probabilities (A_{vk}) in (s^{-1}) and absorption oscillator strengths (f_{kv}) for the Zr IV ion through E1 decay channel are presented in this table. Values in square brackets represent the order of 10. Uncertainties are given in parentheses.

Upper State(v)	Lower State(k)	λ (in Å)	S_{vk} (in a.u.)		A_{Lvk} (in s^{-1})	f_{Lkv}
			L	V		
5P _{1/2}	4D _{3/2}	1219.86	2.04[0]	2.37[0]	1.14(18)[9]	1.27(20)[-1]
5P _{1/2}	5S _{1/2}	2287.38	4.69[0]	5.06[0]	3.97(30)[8]	3.12(24)[-1]
5P _{3/2}	4D _{3/2}	1183.97	3.93[-1]	4.55[-1]	1.20(18)[8]	2.52(38)[-2]
5P _{3/2}	4D _{5/2}	1201.77	3.64[0]	4.21[0]	1.06(16)[9]	1.54(23)[-1]
5P _{3/2}	5S _{1/2}	2164.36	9.40[0]	1.02[1]	4.70(39)[8]	6.60(54)[-1]
5D _{3/2}	5P _{1/2}	1546.17	1.14[1]	1.20[1]	1.56(8)[9]	1.12(6)[0]
5D _{3/2}	5P _{3/2}	1607.95	2.40[0]	2.51[0]	2.92(14)[8]	1.13(5)[-1]
5D _{5/2}	5P _{3/2}	1598.95	2.13[1]	2.25[1]	1.76(9)[9]	1.01(5)[0]
6S _{1/2}	5P _{1/2}	1417.71	1.82[0]	1.90[0]	6.47(27)[8]	1.95(8)[-1]
6S _{1/2}	5P _{3/2}	1469.47	4.06[0]	4.21[0]	1.30(5)[9]	2.10(8)[-1]
6P _{1/2}	4D _{3/2}	588.89	6.51[-2]	7.46[-2]	3.23(46)[8]	8.4(1.2)[-3]
6P _{1/2}	5S _{1/2}	760.16	4.33[-2]	4.84[-2]	1.00(11)[8]	8.66(10)[-3]
6P _{1/2}	5D _{3/2}	4318.29	1.57[1]	1.63[1]	1.97(8)[8]	2.75(11)[-1]
6P _{1/2}	6S _{1/2}	5781.45	1.83[1]	1.91[1]	9.61(40)[7]	4.82(20)[-1]
6P _{3/2}	4D _{3/2}	585.42	1.42[-2]	1.61[-2]	3.59(46)[7]	1.84(24)[-3]
6P _{3/2}	4D _{5/2}	589.75	1.29[-1]	1.47[-1]	3.20(42)[8]	1.11(15)[-2]
6P _{3/2}	5S _{1/2}	754.39	5.35[-2]	6.10[-2]	6.31(86)[7]	1.08(15)[-2]
6P _{3/2}	5D _{3/2}	4138.61	3.00[0]	3.14[0]	2.15(10)[7]	5.51(25)[-2]
6P _{3/2}	5D _{5/2}	4199.45	2.75[1]	2.88[1]	1.88(8)[8]	3.32(15)[-1]
6P _{3/2}	6S _{1/2}	5463.85	3.64[1]	3.80[1]	1.13(5)[8]	1.01(5)[0]
6D _{3/2}	5P _{1/2}	863.64	2.84[-1]	2.86[-1]	2.24(2)[8]	5.00(4)[-2]
6D _{3/2}	5P _{3/2}	882.58	5.01[-2]	5.03[-2]	3.69(1)[7]	4.31(1)[-3]
6D _{3/2}	6P _{1/2}	3577.13	3.40[1]	3.50[1]	3.76(11)[8]	1.44(4)[0]
6D _{3/2}	6P _{3/2}	3710.58	7.17[0]	7.36[0]	7.11(19)[7]	1.47(4)[-1]
6D _{5/2}	5P _{3/2}	881.30	4.73[-1]	4.76[-1]	2.34(1)[8]	4.08(2)[-2]
6D _{5/2}	6P _{3/2}	3687.95	6.39[1]	6.56[1]	4.30(12)[8]	1.32(4)[0]
7S _{1/2}	5P _{1/2}	846.40	1.73[-1]	1.74[-1]	2.89(2)[8]	3.10(3)[-2]
7S _{1/2}	5P _{3/2}	864.59	3.62[-1]	3.63[-1]	5.68(2)[8]	3.18(1)[-2]
7S _{1/2}	6P _{1/2}	3298.81	6.32[0]	6.59[0]	1.78(7)[8]	2.91(12)[-1]
7S _{1/2}	6P _{3/2}	3411.97	1.40[1]	1.45[1]	3.57(13)[8]	3.12(12)[-1]
7P _{1/2}	4D _{3/2}	478.97	1.47[-2]	1.73[-2]	1.35(23)[8]	2.33(39)[-3]
7P _{1/2}	5S _{1/2}	586.42	2.22[-2]	2.38[-2]	1.11(8)[8]	5.74(41)[-3]
7P _{1/2}	5D _{3/2}	1609.50	2.29[-1]	2.18[-1]	5.57(28)[7]	1.08(5)[-2]
7P _{1/2}	6S _{1/2}	1777.13	3.29[-2]	3.84[-2]	5.93(96)[6]	2.81(46)[-3]
7P _{1/2}	6D _{3/2}	9075.84	5.01[1]	5.20[1]	6.79(26)[7]	4.19(16)[-1]
7P _{1/2}	7S _{1/2}	11547.78	4.69[1]	4.83[1]	3.09(9)[7]	6.17(17)[-1]
7P _{3/2}	4D _{3/2}	477.79	3.36[-3]	3.87[-3]	1.56(23)[7]	5.35(77)[-4]
7P _{3/2}	4D _{5/2}	480.66	3.08[-2]	3.56[-2]	1.40(21)[8]	3.24(49)[-3]
7P _{3/2}	5S _{1/2}	584.66	3.27[-2]	3.55[-2]	8.28(70)[7]	8.48(71)[-3]
7P _{3/2}	5D _{3/2}	1596.29	5.21[-2]	5.01[-2]	6.49(26)[6]	2.48(10)[-3]
7P _{3/2}	5D _{5/2}	1605.26	4.58[-1]	4.39[-1]	5.61(23)[7]	1.44(6)[-2]
7P _{3/2}	6S _{1/2}	1761.04	2.24[-2]	2.88[-2]	2.08(56)[6]	1.94(52)[-3]
7P _{3/2}	6D _{3/2}	8671.10	9.62[0]	1.00[1]	7.47(33)[6]	8.42(37)[-2]
7P _{3/2}	6D _{5/2}	8797.22	8.79[1]	9.18[1]	6.54(28)[7]	5.06(22)[-1]
7P _{3/2}	7S _{1/2}	10900.41	9.27[1]	9.56[1]	3.62(12)[7]	1.29(4)[0]
7D _{3/2}	5P _{1/2}	729.14	4.52[-2]	4.39[-2]	5.91(17)[7]	9.42(28)[-3]
7D _{3/2}	5P _{3/2}	741.55	7.23[-3]	6.96[-3]	8.97(34)[6]	7.40(28)[-4]
7D _{3/2}	6P _{1/2}	1902.54	1.21[0]	1.21[0]	8.88(3)[7]	9.64(3)[-2]
7D _{3/2}	6P _{3/2}	1937.55	2.22[-1]	2.22[-1]	1.5449(7)[7]	8.695(4)[-3]
7D _{3/2}	7P _{1/2}	6853.77	7.55[1]	7.71[1]	1.19(2)[8]	1.67(3)[0]
7D _{3/2}	7P _{3/2}	7091.30	1.60[1]	1.63[1]	2.27(4)[7]	1.71(3)[-1]
7D _{5/2}	5P _{3/2}	741.05	7.07[-2]	6.84[-2]	5.87(19)[7]	7.25(24)[-3]
7D _{5/2}	6P _{3/2}	1934.18	2.06[0]	2.06[0]	9.59(1)[7]	8.07(1)[-2]
7D _{5/2}	7P _{3/2}	7046.41	1.42[2]	1.45[2]	1.37(3)[8]	1.53(3)[0]

$8S_{1/2}$	$5P_{1/2}$	700.10	5.41[−2]	5.37[−2]	1.60(1)[8]	1.17(1)[−2]
$8S_{1/2}$	$5P_{3/2}$	712.49	1.12[−1]	1.10[−1]	3.13(4)[8]	1.19(1)[−2]
$8S_{1/2}$	$6P_{1/2}$	1818.06	5.04[−1]	5.15[−1]	8.50(18)[7]	4.21(9)[−2]
$8S_{1/2}$	$6P_{3/2}$	1851.91	1.05[0]	1.06[0]	1.67(3)[8]	4.30(7)[−2]
$8S_{1/2}$	$7P_{1/2}$	6238.26	1.60[1]	1.66[1]	6.66(27)[7]	3.88(16)[−1]
$8S_{1/2}$	$7P_{3/2}$	6445.03	3.52[1]	3.64[1]	1.33(5)[8]	4.14(15)[−1]
$8P_{1/2}$	$4D_{3/2}$	455.75	5.34[−3]	6.48[−3]	5.7(1.2)[7]	8.9(1.8)[−4]
$8P_{1/2}$	$5S_{1/2}$	540.99	1.24[−2]	1.30[−2]	7.91(41)[7]	3.47(18)[−3]
$8P_{1/2}$	$5D_{3/2}$	1240.73	5.17[−2]	4.77[−2]	2.74(21)[7]	3.16(25)[−3]
$8P_{1/2}$	$6S_{1/2}$	1325.84	2.14[−2]	2.38[−2]	9.3(1.0)[6]	2.45(27)[−3]
$8P_{1/2}$	$6D_{3/2}$	3212.52	5.38[−1]	5.14[−1]	1.64(7)[7]	1.27(6)[−2]
$8P_{1/2}$	$7S_{1/2}$	3435.43	2.81[−2]	3.37[−2]	7.0(1.3)[5]	1.24(24)[−3]
$8P_{1/2}$	$7D_{3/2}$	16784.45	1.19[2]	1.24[2]	2.55(11)[7]	5.38(23)[−1]
$8P_{1/2}$	$8S_{1/2}$	20310.35	9.89[1]	1.01[2]	1.20(2)[7]	7.40(15)[−1]
$8P_{3/2}$	$4D_{3/2}$	455.16	1.28[−3]	1.51[−3]	6.9(1.2)[6]	2.14(37)[−4]
$8P_{3/2}$	$4D_{5/2}$	457.47	1.17[−2]	1.39[−2]	6.2(1.1)[7]	1.30(23)[−3]
$8P_{3/2}$	$5S_{1/2}$	540.15	1.92[−2]	2.04[−2]	6.16(39)[7]	5.39(3)[−3]
$8P_{3/2}$	$5D_{3/2}$	1236.33	1.20[−2]	1.12[−2]	3.21(21)[6]	7.35(48)[−4]
$8P_{3/2}$	$5D_{5/2}$	1241.52	1.05[−1]	9.78[−2]	2.77(19)[7]	4.27(29)[−3]
$8P_{3/2}$	$6S_{1/2}$	1320.82	2.46[−2]	2.84[−2]	5.41(80)[6]	2.83(42)[−3]
$8P_{3/2}$	$6D_{3/2}$	3183.19	1.26[−1]	1.22[−1]	1.98(7)[6]	3.00(10)[−3]
$8P_{3/2}$	$6D_{5/2}$	3199.59	1.10[0]	1.06[0]	1.69(6)[7]	1.73(6)[−2]
$8P_{3/2}$	$7S_{1/2}$	3401.92	6.29[−3]	1.02[−2]	8.1(4.4)[4]	2.8(1.5)[−4]
$8P_{3/2}$	$7D_{3/2}$	16013.68	2.29[1]	2.39[1]	2.82(13)[6]	1.09(5)[−1]
$8P_{3/2}$	$7D_{5/2}$	16247.40	2.09[2]	2.18[2]	2.47(11)[7]	6.51(29)[−1]
$8P_{3/2}$	$8S_{1/2}$	19192.52	1.95[2]	1.99[2]	1.40(3)[7]	1.54(4)[0]
$8D_{3/2}$	$5P_{1/2}$	658.67	1.31[−2]	1.23[−2]	2.32(14)[7]	3.02(18)[−3]
$8D_{3/2}$	$5P_{3/2}$	668.77	1.93[−3]	1.79[−3]	3.26(24)[6]	2.19(16)[−4]
$8D_{3/2}$	$6P_{1/2}$	1487.30	2.45[−1]	2.41[−1]	3.78(7)[7]	2.51(4)[−2]
$8D_{3/2}$	$6P_{3/2}$	1508.61	4.26[−2]	4.17[−2]	6.29(14)[6]	2.15(5)[−3]
$8D_{3/2}$	$7P_{1/2}$	3417.04	2.97[0]	2.99[0]	3.78(2)[7]	1.32(1)[−1]
$8D_{3/2}$	$7P_{3/2}$	3475.08	5.56[−1]	5.57[−1]	6.71(2)[6]	1.215(3)[−2]
$8D_{3/2}$	$8P_{1/2}$	11472.29	1.45[2]	1.47[2]	4.85(7)[7]	1.91(3)[0]
$8D_{3/2}$	$8P_{3/2}$	11862.56	3.07[1]	3.11[1]	9.31(12)[6]	1.96(2)[−1]
$8D_{5/2}$	$5P_{3/2}$	668.52	1.95[−2]	1.83[−2]	2.21(15)[7]	2.22(15)[−3]
$8D_{5/2}$	$6P_{3/2}$	1507.35	4.02[−1]	3.93[−1]	3.96(8)[7]	2.02(4)[−2]
$8D_{5/2}$	$7P_{3/2}$	3468.39	5.12[0]	5.13[0]	4.14(1)[7]	1.121(3)[−1]
$8D_{5/2}$	$8P_{3/2}$	11785.04	2.73[2]	2.76[2]	5.63(7)[7]	1.76(2)[0]
$9S_{1/2}$	$5P_{1/2}$	655.99	2.49[−2]	2.45[−2]	8.94(15)[7]	5.77(10)[−3]
$9S_{1/2}$	$5P_{3/2}$	666.01	5.10[−2]	5.00[−2]	1.75(4)[8]	5.81(12)[−3]
$9S_{1/2}$	$6P_{1/2}$	1473.70	1.46[−1]	1.48[−1]	4.64(5)[7]	1.51(2)[−2]
$9S_{1/2}$	$6P_{3/2}$	1494.62	3.00[−1]	3.01[−1]	9.09(5)[7]	1.52(1)[−2]
$9S_{1/2}$	$7P_{1/2}$	3346.08	1.16[0]	1.19[0]	3.12(8)[7]	5.24(14)[−2]
$9S_{1/2}$	$7P_{3/2}$	3401.71	2.39[0]	2.44[0]	6.15(13)[7]	5.33(12)[−2]
$9S_{1/2}$	$8P_{1/2}$	10709.75	3.34[1]	3.46[1]	2.75(11)[7]	4.73(18)[−1]
$9S_{1/2}$	$8P_{3/2}$	10813.09	7.34[1]	7.58[1]	5.88(19)[7]	5.15(17)[−1]
$9P_{1/2}$	$4D_{3/2}$	431.37	2.45[−3]	3.05[−3]	3.09(71)[7]	4.31(99)[−4]
$9P_{1/2}$	$5S_{1/2}$	506.98	7.59[−3]	7.90[−3]	5.90(24)[7]	2.27(9)[−3]
$9P_{1/2}$	$5D_{3/2}$	1075.28	2.05[−2]	1.87[−2]	1.67(15)[7]	1.45(13)[−3]
$9P_{1/2}$	$6S_{1/2}$	1138.63	1.19[−2]	1.30[−2]	8.14(79)[6]	1.58(15)[−3]
$9P_{1/2}$	$6D_{3/2}$	2297.29	1.12[−1]	1.04[−1]	9.33(69)[6]	3.69(27)[−3]
$9P_{1/2}$	$7S_{1/2}$	2409.07	2.49[−2]	2.82[−2]	1.80(24)[6]	1.57(21)[−3]
$9P_{1/2}$	$7D_{3/2}$	5446.84	1.04[0]	1.01[0]	6.51(20)[6]	1.45(4)[−2]
$9P_{1/2}$	$8S_{1/2}$	5772.02	2.38[−2]	3.00[−2]	1.26(31)[5]	6.3(15)[−4]
$9P_{1/2}$	$8D_{3/2}$	27139.20	2.40[2]	2.51[2]	1.21(6)[7]	6.70(32)[−1]
$9P_{1/2}$	$9S_{1/2}$	32636.33	1.85[2]	1.89[2]	5.40(9)[6]	8.63(14)[−1]
$9P_{3/2}$	$4D_{3/2}$	431.02	6.30[−4]	7.56[−4]	3.99(76)[6]	1.11(21)[−4]
$9P_{3/2}$	$4D_{5/2}$	433.09	5.49[−3]	6.64[−3]	3.42(68)[7]	6.4(1.3)[−4]
$9P_{3/2}$	$5S_{1/2}$	506.49	1.21[−2]	1.27[−2]	4.72(25)[7]	3.63(19)[−3]
$9P_{3/2}$	$5D_{3/2}$	1073.09	4.82[−3]	4.44[−3]	1.97(16)[6]	3.41(28)[−4]
$9P_{3/2}$	$5D_{5/2}$	1077.00	4.20[−2]	3.87[−2]	1.70(14)[7]	1.98(16)[−3]
$9P_{3/2}$	$6S_{1/2}$	1136.17	1.53[−2]	1.73[−2]	5.28(66)[6]	2.05(26)[−3]

9P _{3/2}	6D _{3/2}	2287.32	2.68[−2]	2.52[−2]	1.13(7)[6]	8.90(54)[−4]
9P _{3/2}	6D _{5/2}	2295.78	2.32[−1]	2.17[−1]	9.71(62)[6]	5.11(33)[−3]
9P _{3/2}	7S _{1/2}	2398.11	2.27[−2]	2.74[−2]	8.3(1.6)[5]	1.44(28)[−3]
9P _{3/2}	7D _{3/2}	5391.15	2.50[−1]	2.45[−1]	8.08(17)[5]	3.52(7)[−3]
9P _{3/2}	7D _{5/2}	5417.39	2.16[0]	2.11[0]	6.89(17)[6]	2.02(5)[−2]
9P _{3/2}	8D _{3/2}	25810.71	4.61[1]	4.84[1]	1.36(7)[6]	1.36(7)[−1]
9P _{3/2}	8D _{5/2}	26185.44	4.20[2]	4.38[2]	1.19(6)[7]	8.13(38)[−1]
9P _{3/2}	9S _{1/2}	30734.01	3.64[2]	3.70[2]	6.36(9)[6]	1.80(3)[0]
9D _{3/2}	5P _{1/2}	620.51	5.17[−3]	4.72[−3]	1.10(10)[7]	1.27(11)[−3]
9D _{3/2}	5P _{3/2}	629.51	7.08[−4]	6.35[−4]	1.44(15)[6]	8.54(90)[−5]
9D _{3/2}	6P _{1/2}	1306.15	8.77[−2]	8.46[−2]	1.99(7)[7]	1.02(4)[−2]
9D _{3/2}	6P _{3/2}	1322.55	1.47[−2]	1.41[−2]	3.23(14)[6]	8.46(36)[−4]
9D _{3/2}	7P _{1/2}	2591.33	6.40[−1]	6.32[−1]	1.86(2)[7]	3.75(5)[−2]
9D _{3/2}	7P _{3/2}	2624.57	1.14[−1]	1.13[−1]	3.20(5)[6]	3.31(5)[−3]
9D _{3/2}	8P _{1/2}	5542.67	5.96[0]	5.98[0]	1.77(1)[7]	1.63(1)[−1]
9D _{3/2}	8P _{3/2}	5632.20	1.12[0]	1.13[0]	3.19(1)[6]	1.516(4)[−2]
9D _{3/2}	9P _{1/2}	17729.01	2.51[2]	2.53[2]	2.28(2)[7]	2.15(2)[0]
9D _{3/2}	9P _{3/2}	18345.87	5.34[1]	5.38[1]	4.38(4)[6]	2.21(2)[−1]
9D _{5/2}	5P _{3/2}	629.37	7.43[−3]	6.72[−3]	1.01(10)[7]	8.97(87)[−4]
9D _{5/2}	6P _{3/2}	1321.90	1.40[−1]	1.37[−1]	2.05(8)[7]	8.05(32)[−3]
9D _{5/2}	7P _{3/2}	2622.01	1.07[0]	1.05[0]	2.00(3)[7]	3.09(5)[−2]
9D _{5/2}	8P _{3/2}	5620.43	1.03[1]	1.03[1]	1.9615(2)[7]	1.3935(2)[−1]
9D _{5/2}	9P _{3/2}	18221.68	4.74[2]	4.77[2]	2.65(1)[7]	1.98(1)[0]
10S _{1/2}	5P _{1/2}	618.88	1.38[−2]	1.35[−2]	5.90(13)[7]	3.39(8)[−3]
10S _{1/2}	5P _{3/2}	627.80	2.81[−2]	2.74[−2]	1.15(3)[8]	3.40(9)[−3]
10S _{1/2}	6P _{1/2}	1298.78	6.46[−2]	6.49[−2]	2.99(1)[7]	7.55(4)[−3]
10S _{1/2}	6P _{3/2}	1315.00	1.31[−1]	1.31[−1]	5.841(3)[7]	7.572(4)[−3]
10S _{1/2}	7P _{1/2}	2562.48	3.18[−1]	3.25[−1]	1.92(4)[7]	1.89(4)[−2]
10S _{1/2}	7P _{3/2}	2594.98	6.48[−1]	6.58[−1]	3.76(6)[7]	1.90(3)[−2]
10S _{1/2}	8P _{1/2}	5412.36	2.27[0]	2.34[0]	1.45(5)[7]	6.36(20)[−2]
10S _{1/2}	8P _{3/2}	5497.69	4.68[0]	4.78[0]	2.85(6)[7]	6.47(14)[−2]
10S _{1/2}	9P _{1/2}	16461.27	6.06[1]	6.29[1]	1.38(5)[7]	5.59(20)[−1]
10S _{1/2}	9P _{3/2}	16991.74	1.34[2]	1.37[2]	2.76(7)[7]	5.98(16)[−1]
10P _{1/2}	4D _{3/2}	416.88	1.45[−3]	1.81[−3]	2.03(48)[7]	2.64(63)[−4]
10P _{1/2}	5S _{1/2}	487.08	4.83[−3]	5.00[−3]	4.23(15)[7]	1.51(5)[−3]
10P _{1/2}	5D _{3/2}	989.54	1.01[−2]	9.12[−3]	1.06(11)[7]	7.75(77)[−4]
10P _{1/2}	6S _{1/2}	1042.94	6.91[−3]	7.53[−3]	6.17(55)[6]	1.01(9)[−3]
10P _{1/2}	6D _{3/2}	1938.47	4.17[−2]	3.80[−2]	5.80(53)[6]	1.64(15)[−3]
10P _{1/2}	7S _{1/2}	2017.46	1.37[−2]	1.57[−2]	1.69(23)[6]	1.03(14)[−3]
10P _{1/2}	7D _{3/2}	3785.49	1.95[−1]	1.84[−1]	3.64(20)[6]	3.91(22)[−3]
10P _{1/2}	8S _{1/2}	3939.74	2.86[−2]	3.44[−2]	4.74(91)[5]	1.10(21)[−3]
10P _{1/2}	8D _{3/2}	8516.33	1.73[0]	1.71[0]	2.84(4)[6]	1.54(2)[−2]
10P _{1/2}	9S _{1/2}	8991.59	2.37[−2]	3.37[−2]	3.3(1.3)[4]	4.0(1.5)[−4]
10P _{1/2}	9D _{3/2}	41374.25	4.33[2]	4.58[2]	6.19(36)[6]	7.94(46)[−1]
10P _{3/2}	4D _{3/2}	416.63	4.88[−4]	5.76[−4]	3.42(59)[6]	8.9(1.5)[−5]
10P _{3/2}	4D _{5/2}	418.56	2.57[−3]	3.21[−3]	1.78(42)[7]	3.11(74)[−4]
10P _{3/2}	5S _{1/2}	486.74	7.96[−3]	8.32[−3]	3.50(16)[7]	2.48(11)[−3]
10P _{3/2}	5D _{3/2}	988.13	2.42[−3]	2.21[−3]	1.27(11)[6]	1.86(17)[−4]
10P _{3/2}	5D _{5/2}	991.44	2.11[−2]	1.93[−2]	1.10(10)[7]	1.08(10)[−3]
10P _{3/2}	6S _{1/2}	1041.37	9.51[−3]	1.07[−2]	4.26(50)[6]	1.39(16)[−3]
10P _{3/2}	6D _{3/2}	1933.04	1.02[−2]	9.49[−3]	7.18(54)[5]	4.02(30)[−4]
10P _{3/2}	6D _{5/2}	1939.07	8.86[−2]	8.17[−2]	6.16(49)[6]	2.31(19)[−3]
10P _{3/2}	7S _{1/2}	2011.58	1.53[−2]	1.83[−2]	9.5(1.8)[5]	1.15(22)[−3]
10P _{3/2}	7D _{3/2}	3764.81	4.90[−2]	4.69[−2]	4.65(20)[5]	9.89(43)[−4]
10P _{3/2}	7D _{5/2}	3777.59	4.21[−1]	3.99[−1]	3.96(21)[6]	5.65(30)[−3]
10P _{3/2}	8S _{1/2}	3917.35	1.99[−2]	2.77[−2]	1.68(60)[5]	7.7(2.8)[−4]
10P _{3/2}	8D _{3/2}	8412.42	4.35[−1]	4.32[−1]	3.70(2)[5]	3.92(2)[−3]
10P _{3/2}	8D _{5/2}	8451.84	3.74[0]	3.66[0]	3.14(7)[6]	2.24(5)[−2]
10P _{3/2}	9S _{1/2}	8875.83	7.83[−3]	7.31[−3]	5.3(7.0)[3]	1.3(1.7)[−4]
10P _{3/2}	9D _{3/2}	39031.88	8.32[1]	8.79[1]	7.08(40)[5]	1.62(9)[−1]
10P _{3/2}	9D _{5/2}	39606.22	7.59[2]	7.93[2]	6.18(28)[6]	9.70(44)[−1]
10D _{3/2}	5P _{1/2}	597.21	2.47[−3]	2.20[−3]	5.87(66)[6]	6.28(71)[−4]

$10D_{3/2}$	$5P_{3/2}$	605.50	3.20[−4]	2.76[−4]	7.3(1.1)[5]	4.02(58)[−5]
$10D_{3/2}$	$6P_{1/2}$	1206.84	4.17[−2]	3.94[−2]	1.20(7)[7]	5.24(29)[−3]
$10D_{3/2}$	$6P_{3/2}$	1220.83	6.86[−3]	6.42[−3]	1.91(12)[6]	4.26(28)[−4]
$10D_{3/2}$	$7P_{1/2}$	2227.66	2.40[−1]	2.31[−1]	1.10(4)[7]	1.63(6)[−2]
$10D_{3/2}$	$7P_{3/2}$	2252.18	4.18[−2]	4.02[−2]	1.85(7)[6]	1.41(5)[−3]
$10D_{3/2}$	$8P_{1/2}$	4108.17	1.32[0]	1.29[0]	9.66(21)[6]	4.89(10)[−2]
$10D_{3/2}$	$8P_{3/2}$	4157.14	2.39[−1]	2.35[−1]	1.69(3)[6]	4.37(8)[−3]
$10D_{3/2}$	$9P_{1/2}$	8374.94	1.07[1]	1.06[1]	9.26(11)[6]	1.95(2)[−1]
$10D_{3/2}$	$9P_{3/2}$	8510.11	2.03[0]	2.02[0]	1.67(1)[6]	1.81(1)[−2]
$10D_{5/2}$	$5P_{3/2}$	605.40	3.43[−3]	3.01[−3]	5.23(66)[6]	4.31(54)[−4]
$10D_{5/2}$	$6P_{3/2}$	1220.42	6.54[−2]	6.15[−2]	1.22(7)[7]	4.07(25)[−3]
$10D_{5/2}$	$7P_{3/2}$	2250.78	3.91[−1]	3.76[−1]	1.16(4)[7]	1.32(5)[−2]
$10D_{5/2}$	$8P_{3/2}$	4152.37	2.21[0]	2.16[0]	1.04(3)[7]	4.05(10)[−2]
$10D_{5/2}$	$9P_{3/2}$	8490.14	1.86[1]	1.83[1]	1.02(2)[7]	1.66(3)[−1]

Table 3: The line strengths (S_{vk}) (in a.u.) from both the L and V gauge expressions, wavelengths (λ) (in Å), transition probabilities (A_{vk}) in (s^{-1}) and absorption oscillator strengths (f_{kv}) for the Nb V ion through E1 decay channel are presented in this table. Values in square brackets represent the order of 10. Uncertainties are given in parentheses.

Upper State(v)	Lower State(k)	λ (in Å)	S_{vk} (in a.u.)		A_{Lvk} (in s^{-1})	f_{Lkv}
			L	V		
$5P_{1/2}$	$4D_{3/2}$	774.02	1.34[0]	1.45[0]	2.94(23)[9]	1.32(10)[−1]
$5P_{1/2}$	$5S_{1/2}$	1877.38	3.71[0]	3.88[0]	5.67(26)[8]	3.00(14)[−1]
$5P_{3/2}$	$4D_{3/2}$	753.01	2.56[−1]	2.76[−1]	3.04(23)[8]	2.58(20)[−2]
$5P_{3/2}$	$4D_{5/2}$	763.75	2.38[0]	2.57[0]	2.71(20)[9]	1.58(12)[−1]
$5P_{3/2}$	$5S_{1/2}$	1758.38	7.43[0]	7.82[0]	6.92(36)[8]	6.42(33)[−1]
$5D_{3/2}$	$5P_{1/2}$	1212.14	9.04[0]	9.33[0]	2.57(8)[9]	1.13(4)[0]
$5D_{3/2}$	$5P_{3/2}$	1267.52	1.90[0]	1.95[0]	4.72(13)[8]	1.14(3)[−1]
$5D_{5/2}$	$5P_{3/2}$	1258.84	1.70[1]	1.75[1]	2.87(9)[9]	1.02(3)[0]
$6S_{1/2}$	$5P_{1/2}$	1007.04	1.28[0]	1.32[0]	1.27(4)[9]	1.92(6)[−1]
$6S_{1/2}$	$5P_{3/2}$	1044.97	2.88[0]	2.95[0]	2.55(6)[9]	2.09(5)[−1]
$6P_{1/2}$	$4D_{3/2}$	399.19	5.03[−2]	5.55[−2]	8.01(81)[8]	9.57(96)[−3]
$6P_{1/2}$	$5S_{1/2}$	572.81	5.92[−2]	6.37[−2]	3.19(23)[8]	1.57(12)[−2]
$6P_{1/2}$	$5D_{3/2}$	2576.49	9.64[0]	9.85[0]	5.71(12)[8]	2.84(6)[−1]
$6P_{1/2}$	$6S_{1/2}$	4543.35	1.39[1]	1.42[1]	1.50(3)[8]	4.64(10)[−1]
$6P_{3/2}$	$4D_{3/2}$	396.79	1.10[−2]	1.20[−2]	8.94(78)[7]	2.11(19)[−3]
$6P_{3/2}$	$4D_{5/2}$	399.75	1.01[−1]	1.11[−1]	8.03(72)[8]	1.28(12)[−2]
$6P_{3/2}$	$5S_{1/2}$	567.88	8.03[−2]	8.76[−2]	2.22(20)[8]	2.15(19)[−2]
$6P_{3/2}$	$5D_{3/2}$	2479.59	1.83[0]	1.88[0]	6.09(15)[7]	5.61(14)[−2]
$6P_{3/2}$	$5D_{5/2}$	2513.52	1.68[1]	1.73[1]	5.37(13)[8]	3.39(8)[−1]
$6P_{3/2}$	$6S_{1/2}$	4250.44	2.76[1]	2.82[1]	1.82(5)[8]	9.85(25)[−1]
$6D_{3/2}$	$5P_{1/2}$	633.04	1.05[−1]	1.01[−1]	2.10(9)[8]	2.52(10)[−2]
$6D_{3/2}$	$5P_{3/2}$	647.82	1.64[−2]	1.56[−2]	3.06(16)[7]	1.92(10)[−3]
$6D_{3/2}$	$6P_{1/2}$	2727.98	2.72[1]	2.76[1]	6.78(9)[8]	1.51(2)[0]
$6D_{3/2}$	$6P_{3/2}$	2845.74	5.72[0]	5.78[0]	1.26(1)[8]	1.53(2)[−1]
$6D_{5/2}$	$5P_{3/2}$	646.72	1.62[−1]	1.54[−1]	2.02(10)[8]	1.90(9)[−2]
$6D_{5/2}$	$6P_{3/2}$	2824.68	5.11[1]	5.16[1]	7.65(9)[8]	1.37(2)[0]
$7S_{1/2}$	$5P_{1/2}$	604.08	1.29[−1]	1.29[−1]	5.94(2)[8]	3.25(1)[−2]
$7S_{1/2}$	$5P_{3/2}$	617.53	2.72[−1]	2.70[−1]	1.17(1)[9]	3.35(3)[−2]
$7S_{1/2}$	$6P_{1/2}$	2260.93	4.18[0]	4.33[0]	3.66(13)[8]	2.81(10)[−1]
$7S_{1/2}$	$6P_{3/2}$	2341.22	9.35[0]	9.65[0]	7.38(23)[8]	3.03(10)[−1]
$7P_{1/2}$	$4D_{3/2}$	326.81	9.14[−3]	1.23[−2]	2.65(84)[8]	2.12(68)[−3]
$7P_{1/2}$	$5S_{1/2}$	434.68	2.83[−2]	2.93[−2]	3.49(13)[8]	9.87(36)[−3]
$7P_{1/2}$	$5D_{3/2}$	1060.53	2.23[−1]	2.10[−1]	1.89(11)[8]	1.59(9)[−2]
$7P_{1/2}$	$6S_{1/2}$	1290.49	6.01[−2]	6.62[−2]	2.83(28)[7]	7.08(69)[−3]
$7P_{1/2}$	$6D_{3/2}$	5312.68	3.02[1]	3.10[1]	2.04(5)[8]	4.31(11)[−1]
$7P_{1/2}$	$7S_{1/2}$	8888.49	3.46[1]	3.50[1]	5.00(5)[7]	5.92(6)[−1]
$7P_{3/2}$	$4D_{3/2}$	325.96	2.27[−3]	2.78[−3]	3.31(72)[7]	5.3(1.2)[−4]
$7P_{3/2}$	$4D_{5/2}$	327.95	2.01[−2]	2.48[−2]	2.88(64)[8]	3.10(69)[−3]

$7P_{3/2}$	$5S_{1/2}$	433.17	4.38[−2]	4.58[−2]	2.73(13)[8]	1.54(7)[−2]
$7P_{3/2}$	$5D_{3/2}$	1051.59	4.86[−2]	4.62[−2]	2.12(11)[7]	3.51(18)[−3]
$7P_{3/2}$	$5D_{5/2}$	1057.64	4.32[−1]	4.10[−1]	1.85(10)[8]	2.07(11)[−2]
$7P_{3/2}$	$6S_{1/2}$	1277.27	6.00[−2]	6.88[−2]	1.46(21)[7]	7.1(1.0)[−3]
$7P_{3/2}$	$6D_{3/2}$	5095.67	5.74[0]	5.92[0]	2.20(7)[7]	8.56(26)[−2]
$7P_{3/2}$	$6D_{5/2}$	5164.62	5.26[1]	5.42[1]	1.93(6)[8]	5.16(15)[−1]
$7P_{3/2}$	$7S_{1/2}$	8297.31	6.85[1]	6.94[1]	6.07(8)[7]	1.25(2)[0]
$7D_{3/2}$	$5P_{1/2}$	508.88	7.89[−3]	6.74[−3]	3.03(46)[7]	2.35(36)[−3]
$7D_{3/2}$	$5P_{3/2}$	518.39	8.58[−4]	6.86[−4]	3.12(66)[6]	1.26(27)[−4]
$7D_{3/2}$	$6P_{1/2}$	1329.80	5.85[−1]	5.69[−2]	1.26(3)[8]	6.68(19)[−2]
$7D_{3/2}$	$6P_{3/2}$	1357.18	1.00[−1]	9.72[−2]	2.03(7)[7]	5.62(18)[−3]
$7D_{3/2}$	$7P_{1/2}$	5071.20	6.03[1]	6.08[1]	2.34(2)[8]	1.81(1)[0]
$7D_{3/2}$	$7P_{3/2}$	5286.08	1.27[1]	1.28[1]	4.37(2)[7]	1.83(1)[−1]
$7D_{5/2}$	$5P_{3/2}$	517.99	9.96[−3]	8.22[−3]	2.42(44)[7]	1.46(27)[−3]
$7D_{5/2}$	$6P_{3/2}$	1354.44	9.49[−1]	9.20[−1]	1.29(4)[8]	5.32(17)[−2]
$7D_{5/2}$	$7P_{3/2}$	5244.75	1.13[2]	1.14[2]	2.66(1)[8]	1.64(1)[0]
$8S_{1/2}$	$5P_{1/2}$	498.28	4.13[−2]	4.06[−2]	3.38(6)[8]	1.26(2)[−2]
$8S_{1/2}$	$5P_{3/2}$	507.40	8.54[−2]	8.35[−2]	6.63(15)[8]	1.28(3)[−2]
$8S_{1/2}$	$6P_{1/2}$	1259.80	3.57[−1]	3.63[−1]	1.81(3)[8]	4.31(6)[−2]
$8S_{1/2}$	$6P_{3/2}$	1284.34	7.50[−1]	7.57[−1]	3.59(3)[8]	4.43(4)[−2]
$8S_{1/2}$	$7P_{1/2}$	4184.50	1.02[1]	1.06[1]	1.41(5)[8]	3.71(14)[−1]
$8S_{1/2}$	$7P_{3/2}$	4329.74	2.28[1]	2.36[1]	2.84(9)[8]	4.00(13)[−1]
$8P_{1/2}$	$4D_{3/2}$	307.43	2.44[−3]	4.19[−3]	8.5(5.3)[7]	6.0(3.7)[−4]
$8P_{1/2}$	$5S_{1/2}$	394.99	1.69[−2]	1.72[−2]	2.77(5)[8]	6.49(12)[−3]
$8P_{1/2}$	$5D_{3/2}$	823.88	5.21[−2]	4.76[−2]	9.44(84)[7]	4.80(43)[−3]
$8P_{1/2}$	$6S_{1/2}$	944.92	2.86[−2]	3.06[−2]	3.43(24)[7]	4.60(32)[−3]
$8P_{1/2}$	$6D_{3/2}$	2082.48	5.58[−1]	5.32[−1]	6.26(29)[7]	2.03(9)[−2]
$8P_{1/2}$	$7S_{1/2}$	2433.04	7.52[−2]	8.23[−2]	5.29(48)[6]	4.70(43)[−3]
$8P_{1/2}$	$7D_{3/2}$	9672.58	7.10[1]	7.34[1]	7.95(26)[7]	5.58(18)[−1]
$8P_{1/2}$	$8S_{1/2}$	15199.75	7.16[1]	7.17[1]	2.065(4)[7]	7.15(1)[−1]
$8P_{3/2}$	$4D_{3/2}$	306.99	6.97[−4]	1.01[−3]	1.22(50)[7]	1.72(71)[−4]
$8P_{3/2}$	$4D_{5/2}$	308.64	6.12[−3]	8.97[−3]	1.05(45)[8]	1.00(42)[−3]
$8P_{3/2}$	$5S_{1/2}$	394.27	2.65[−2]	2.73[−2]	2.19(6)[8]	1.02(3)[−2]
$8P_{3/2}$	$5D_{3/2}$	820.74	1.16[−2]	1.07[−2]	1.06(8)[7]	1.08(9)[−3]
$8P_{3/2}$	$5D_{5/2}$	824.33	1.03[−1]	9.47[−2]	9.29(75)[7]	6.31(51)[−3]
$8P_{3/2}$	$6S_{1/2}$	940.79	3.72[−2]	4.08[−2]	2.27(21)[7]	6.01(56)[−3]
$8P_{3/2}$	$6D_{3/2}$	2062.53	1.24[−1]	1.19[−1]	7.15(28)[6]	4.56(18)[−3]
$8P_{3/2}$	$6D_{5/2}$	2073.40	1.09[0]	1.05[0]	6.21(25)[7]	2.67(11)[−2]
$8P_{3/2}$	$7S_{1/2}$	2405.86	5.58[−2]	6.53[−2]	2.03(33)[6]	3.52(58)[−3]
$8P_{3/2}$	$7D_{3/2}$	9256.70	1.35[1]	1.40[1]	8.62(30)[6]	1.11(4)[−1]
$8P_{3/2}$	$7D_{5/2}$	9380.50	1.24[2]	1.28[2]	7.59(25)[7]	6.67(22)[−1]
$8P_{3/2}$	$8S_{1/2}$	14197.42	1.41[2]	1.41[2]	2.50(1)[7]	1.510(4)[0]
$8D_{3/2}$	$5P_{1/2}$	468.43	7.18[−4]	4.58[−4]	3.5(1.4)[6]	2.33(94)[−4]
$8D_{3/2}$	$5P_{3/2}$	476.00	2.50[−5]	6.25[−6]	1.2(1.2)[5]	4.0(4.0)[−6]
$8D_{3/2}$	$6P_{1/2}$	1042.70	9.38[−2]	8.78[−2]	4.19(27)[7]	1.37(9)[−2]
$8D_{3/2}$	$6P_{3/2}$	1058.70	1.45[−2]	1.34[−2]	6.20(48)[6]	1.04(8)[−3]
$8D_{3/2}$	$7P_{1/2}$	2401.87	1.54[0]	1.52[0]	5.62(8)[7]	9.72(13)[−2]
$8D_{3/2}$	$7P_{3/2}$	2446.65	2.72[−1]	2.67[−1]	9.42(19)[6]	8.45(17)[−3]
$8D_{3/2}$	$8P_{1/2}$	8491.33	1.15[2]	1.16[2]	9.52(9)[7]	2.06(2)[0]
$8D_{3/2}$	$8P_{3/2}$	8839.98	2.44[1]	2.45[1]	1.79(1)[7]	2.10(1)[−1]
$8D_{5/2}$	$5P_{3/2}$	475.80	5.76[−4]	2.86[−4]	1.8(1.1)[6]	9.2(5.4)[−5]
$8D_{5/2}$	$6P_{3/2}$	1057.71	1.42[−1]	1.31[−1]	4.04(30)[7]	1.02(7)[−2]
$8D_{5/2}$	$7P_{3/2}$	2441.38	2.55[0]	2.50[0]	5.91(12)[7]	7.93(16)[−2]
$8D_{5/2}$	$8P_{3/2}$	8771.50	2.17[2]	2.18[2]	1.1(4.4)[8]	1.9(7.5)[0]
$9S_{1/2}$	$5P_{1/2}$	463.54	1.92[−2]	1.88[−2]	1.96(5)[8]	6.30(16)[−3]
$9S_{1/2}$	$5P_{3/2}$	470.95	3.94[−2]	3.82[−2]	3.83(12)[8]	6.36(20)[−3]
$9S_{1/2}$	$6P_{1/2}$	1018.77	1.05[−1]	1.06[−1]	1.01(1)[8]	1.57(1)[−2]
$9S_{1/2}$	$6P_{3/2}$	1034.03	2.18[−1]	2.18[−1]	1.997(3)[8]	1.601(2)[−2]
$9S_{1/2}$	$7P_{1/2}$	2278.56	8.00[−1]	8.20[−1]	6.85(18)[7]	5.33(14)[−2]
$9S_{1/2}$	$7P_{3/2}$	2318.83	1.68[0]	1.70[0]	1.36(2)[8]	5.49(8)[−2]
$9S_{1/2}$	$8P_{1/2}$	7127.67	2.11[1]	2.21[1]	5.91(26)[7]	4.51(20)[−1]
$9S_{1/2}$	$8P_{3/2}$	7371.72	4.73[1]	4.88[1]	1.20(4)[8]	4.88(15)[−1]

$9P_{1/2}$	$4D_{3/2}$	291.12	6.86[−4]	1.73[−3]	2.8(3.3)[7]	1.8(2.1)[−4]
$9P_{1/2}$	$5S_{1/2}$	368.48	1.91[−2]	1.91[−2]	3.86(1)[8]	7.86(1)[−3]
$9P_{1/2}$	$5D_{3/2}$	716.36	2.14[−2]	1.92[−2]	5.89(62)[7]	2.27(24)[−3]
$9P_{1/2}$	$6S_{1/2}$	806.14	1.53[−2]	1.61[−2]	2.95(16)[7]	2.88(16)[−3]
$9P_{1/2}$	$6D_{3/2}$	1509.72	1.25[−1]	1.16[−1]	3.67(27)[7]	6.27(46)[−3]
$9P_{1/2}$	$7S_{1/2}$	1685.81	3.97[−2]	4.24[−2]	8.40(57)[6]	3.58(24)[−3]
$9P_{1/2}$	$7D_{3/2}$	3501.83	1.14[0]	1.12[0]	2.69(5)[7]	2.47(5)[−2]
$9P_{1/2}$	$8S_{1/2}$	4032.74	1.04[−1]	1.10[−1]	1.61(9)[6]	3.92(22)[−3]
$9P_{1/2}$	$8D_{3/2}$	15524.92	1.43[2]	1.49[2]	3.86(17)[7]	6.98(31)[−1]
$9P_{1/2}$	$9S_{1/2}$	23876.94	1.31[2]	1.31[2]	9.74(2)[6]	8.32(1)[−1]
$9P_{3/2}$	$4D_{3/2}$	290.83	2.46[−4]	4.49[−4]	5.1(3.6)[6]	6.4(4.5)[−5]
$9P_{3/2}$	$4D_{5/2}$	292.31	2.13[−3]	3.96[−3]	4.3(3.1)[7]	3.7(2.7)[−4]
$9P_{3/2}$	$5S_{1/2}$	368.00	1.33[−2]	1.35[−2]	1.35(3)[8]	5.48(11)[−3]
$9P_{3/2}$	$5D_{3/2}$	714.57	4.82[−3]	4.37[−3]	6.69(64)[6]	5.12(49)[−4]
$9P_{3/2}$	$5D_{5/2}$	717.29	4.25[−2]	3.85[−2]	5.84(57)[7]	3.00(29)[−3]
$9P_{3/2}$	$6S_{1/2}$	803.88	2.14[−2]	2.30[−2]	2.08(16)[7]	4.04(30)[−3]
$9P_{3/2}$	$6D_{3/2}$	1501.79	2.83[−2]	2.65[−2]	4.24(28)[6]	1.43(9)[−3]
$9P_{3/2}$	$6D_{5/2}$	1507.54	2.49[−1]	2.32[−1]	3.67(25)[7]	8.35(57)[−3]
$9P_{3/2}$	$7S_{1/2}$	1675.92	4.47[−2]	4.98[−2]	4.81(53)[6]	4.05(45)[−3]
$9P_{3/2}$	$7D_{3/2}$	3459.45	2.59[−1]	2.54[−1]	3.17(7)[6]	5.69(12)[−3]
$9P_{3/2}$	$7D_{5/2}$	3476.60	2.28[0]	2.22[0]	2.74(7)[7]	3.31(9)[−2]
$9P_{3/2}$	$8S_{1/2}$	3976.63	5.18[−2]	6.40[−2]	4.18(92)[5]	1.98(44)[−3]
$9P_{3/2}$	$8D_{3/2}$	14725.11	2.70[1]	2.80[1]	4.29(16)[6]	1.39(5)[−1]
$9P_{3/2}$	$8D_{5/2}$	14919.13	2.47[2]	2.55[2]	3.77(13)[7]	8.38(28)[−1]
$9P_{3/2}$	$9S_{1/2}$	22036.11	2.57[2]	2.53[2]	1.22(2)[7]	1.77(3)[0]
$9D_{3/2}$	$5P_{3/2}$	446.02	1.16[−5]	2.81[−5]	6.6(7.4)[4]	2.0(2.2)[−6]
$9D_{3/2}$	$6P_{1/2}$	908.87	2.82[−2]	2.56[−2]	1.90(18)[7]	4.71(44)[−3]
$9D_{3/2}$	$6P_{3/2}$	921.00	4.03[−3]	3.59[−3]	2.61(30)[6]	3.32(38)[−4]
$9D_{3/2}$	$7P_{1/2}$	1793.52	2.75[−1]	2.68[−1]	2.42(6)[7]	2.33(6)[−2]
$9D_{3/2}$	$7P_{3/2}$	1818.37	4.56[−2]	4.38[−2]	3.84(16)[6]	1.91(8)[−3]
$9D_{3/2}$	$8P_{1/2}$	3861.18	3.13[0]	3.18[0]	2.76(4)[7]	1.23(2)[−1]
$9D_{3/2}$	$8P_{3/2}$	3931.69	5.67[−1]	5.65[0]	4.73(2)[6]	1.096(4)[−2]
$9D_{3/2}$	$9P_{1/2}$	13019.37	1.96[2]	2.02[2]	4.50(15)[7]	2.29(7)[0]
$9D_{3/2}$	$9P_{3/2}$	13640.71	4.25[1]	4.30[1]	8.47(11)[6]	2.36(3)[−1]
$9D_{5/2}$	$6P_{3/2}$	920.50	4.04[−2]	3.61[−2]	1.75(19)[7]	3.33(37)[−3]
$9D_{5/2}$	$7P_{3/2}$	1816.42	4.36[−1]	4.17[−1]	2.46(11)[7]	1.82(8)[−2]
$9D_{5/2}$	$8P_{3/2}$	3922.57	5.28[0]	5.23[0]	2.96(3)[7]	1.02(1)[−1]
$9D_{5/2}$	$9P_{3/2}$	13531.61	3.78[2]	3.81[2]	5.15(5)[7]	2.12(2)[0]
$10S_{1/2}$	$5P_{1/2}$	436.74	1.06[−2]	1.02[−2]	1.29(4)[8]	3.68(11)[−3]
$10S_{1/2}$	$5P_{3/2}$	443.30	2.15[−2]	2.08[−2]	2.50(9)[8]	3.69(13)[−3]
$10S_{1/2}$	$6P_{1/2}$	897.68	4.59[−2]	4.61[−2]	6.43(2)[7]	7.77(3)[−3]
$10S_{1/2}$	$6P_{3/2}$	909.51	9.45[−2]	9.38[−2]	1.27(1)[8]	7.89(6)[−3]
$10S_{1/2}$	$7P_{1/2}$	1750.46	2.20[−1]	2.26[−1]	4.16(11)[7]	1.91(5)[−2]
$10S_{1/2}$	$7P_{3/2}$	1774.13	4.60[−1]	4.60[−1]	8.34(0)[7]	1.97(0)[−2]
$10S_{1/2}$	$8P_{1/2}$	3666.98	1.53[0]	1.60[0]	3.14(14)[7]	6.33(27)[−2]
$10S_{1/2}$	$8P_{3/2}$	3730.52	3.26[0]	3.26[0]	6.35(1)[7]	6.63(1)[−2]
$10S_{1/2}$	$9P_{1/2}$	11046.79	3.87[1]	4.13[1]	2.91(19)[7]	5.33(35)[−1]
$10S_{1/2}$	$9P_{3/2}$	11490.90	8.96[1]	9.15[1]	5.98(12)[7]	5.92(12)[−1]
$10P_{1/2}$	$5S_{1/2}$	353.07	7.48[−3]	5.18[−3]	1.72(58)[8]	3.2(11)[−3]
$10P_{1/2}$	$5D_{3/2}$	660.34	1.16[−2]	1.03[−2]	4.07(46)[7]	1.33(15)[−3]
$10P_{1/2}$	$6S_{1/2}$	735.89	9.60[−3]	1.01[−2]	2.44(13)[7]	1.98(11)[−3]
$10P_{1/2}$	$6D_{3/2}$	1280.73	5.13[−2]	4.72[−2]	2.48(20)[7]	3.04(25)[−3]
$10P_{1/2}$	$7S_{1/2}$	1405.25	2.21[−2]	2.37[−2]	8.08(54)[6]	2.39(16)[−3]
$10P_{1/2}$	$7D_{3/2}$	2475.27	2.42[−1]	2.39[−1]	1.61(2)[7]	7.42(9)[−3]
$10P_{1/2}$	$8S_{1/2}$	2729.25	6.29[−2]	6.54[−2]	3.13(12)[6]	3.50(14)[−3]
$10P_{1/2}$	$8D_{3/2}$	5469.16	1.94[0]	2.09[0]	1.20(9)[7]	2.70(20)[−2]
$10P_{1/2}$	$9S_{1/2}$	6237.82	1.86[−1]	1.73[−1]	7.76(54)[5]	4.53(32)[−3]
$10P_{1/2}$	$9D_{3/2}$	24025.60	2.62[2]	2.88[2]	1.91(19)[7]	8.27(82)[−1]
$10P_{3/2}$	$4D_{3/2}$	281.10	9.22[−5]	2.28[−4]	2.1(2.4)[6]	2.5(2.9)[−5]
$10P_{3/2}$	$4D_{5/2}$	282.48	7.84[−4]	2.02[−3]	1.8(2.1)[7]	1.4(1.7)[−4]
$10P_{3/2}$	$5S_{1/2}$	352.57	1.30[−2]	8.76[−3]	1.50(54)[8]	5.6(2.0)[−3]
$10P_{3/2}$	$5D_{3/2}$	658.59	2.64[−3]	2.37[−3]	4.68(49)[6]	3.05(32)[−4]

$10P_{3/2}$	$5D_{5/2}$	660.90	2.33[−2]	2.09[−2]	4.10(44)[7]	1.79(19)[−3]
$10P_{3/2}$	$6S_{1/2}$	733.72	1.39[−2]	1.50[−2]	1.79(13)[7]	2.89(21)[−3]
$10P_{3/2}$	$6D_{3/2}$	1274.17	1.19[−2]	1.10[−2]	2.91(22)[6]	7.09(55)[−4]
$10P_{3/2}$	$6D_{5/2}$	1278.31	1.04[−1]	9.58[−2]	2.53(21)[7]	4.13(35)[−3]
$10P_{3/2}$	$7S_{1/2}$	1397.36	2.73[−2]	3.05[−2]	5.06(58)[6]	2.96(34)[−3]
$10P_{3/2}$	$7D_{3/2}$	2450.91	5.83[−2]	5.62[−2]	2.00(7)[6]	1.81(6)[−3]
$10P_{3/2}$	$7D_{5/2}$	2459.51	5.09[−1]	4.86[−1]	1.73(8)[7]	1.05(5)[−2]
$10P_{3/2}$	$8S_{1/2}$	2699.66	5.66[−2]	6.68[−2]	1.46(25)[6]	3.18(55)[−3]
$10P_{3/2}$	$8D_{3/2}$	5351.62	4.86[−1]	4.91[−1]	1.61(2)[6]	6.90(7)[−3]
$10P_{3/2}$	$8D_{5/2}$	5377.03	4.26[0]	4.23[0]	1.39(1)[7]	4.01(2)[−2]
$10P_{3/2}$	$9S_{1/2}$	6085.38	3.29[−2]	5.75[−2]	7.4(4.8)[4]	8.2(5.3)[−4]
$10P_{3/2}$	$9D_{3/2}$	21911.52	4.86[1]	5.11[1]	2.34(12)[6]	1.69(9)[−1]
$10P_{3/2}$	$9D_{5/2}$	22198.99	4.45[2]	4.61[2]	2.06(7)[7]	1.01(4)[0]
$10D_{3/2}$	$5P_{1/2}$	421.63	3.36[−5]	9.03[−5]	2.3(2.9)[5]	1.2(1.6)[−5]
$10D_{3/2}$	$5P_{3/2}$	427.75	4.36[−5]	6.72[−5]	2.8(1.4)[5]	7.7(3.8)[−6]
$10D_{3/2}$	$6P_{1/2}$	836.10	1.15[−2]	1.03[−2]	10.0(1.1)[6]	2.09(23)[−3]
$10D_{3/2}$	$6P_{3/2}$	846.35	1.55[−3]	1.33[−3]	1.30(19)[6]	1.39(21)[−4]
$10D_{3/2}$	$7P_{1/2}$	1530.62	8.92[−2]	8.76[−2]	1.26(2)[7]	8.85(15)[−3]
$10D_{3/2}$	$7P_{3/2}$	1548.69	1.42[−2]	1.36[−2]	1.93(8)[6]	6.96(28)[−4]
$10D_{3/2}$	$8P_{1/2}$	2818.87	5.67[−1]	5.99[−1]	1.28(7)[7]	3.06(17)[−2]
$10D_{3/2}$	$8P_{3/2}$	2856.26	9.80[−2]	9.98[−2]	2.13(4)[6]	2.60(5)[−3]
$10D_{3/2}$	$9P_{1/2}$	5794.65	5.43[0]	6.08[0]	1.41(17)[7]	1.42(17)[−1]
$10D_{3/2}$	$9P_{3/2}$	5914.56	9.98[−1]	1.06[0]	2.44(15)[6]	1.28(8)[−2]
$10D_{5/2}$	$5P_{3/2}$	427.67	1.64[−4]	3.06[−4]	7.1(5.2)[5]	2.9(2.1)[−5]
$10D_{5/2}$	$6P_{3/2}$	846.04	1.58[−2]	1.37[−2]	8.8(1.2)[6]	1.42(20)[−3]
$10D_{5/2}$	$7P_{3/2}$	1547.66	1.38[−1]	1.31[−1]	1.25(6)[7]	6.75(34)[−3]
$10D_{5/2}$	$8P_{3/2}$	2852.75	9.29[−1]	9.27[−1]	1.352(3)[7]	2.47(1)[−2]
$10D_{5/2}$	$9P_{3/2}$	5899.51	9.28[0]	9.59[0]	1.53(5)[7]	1.19(4)[−1]

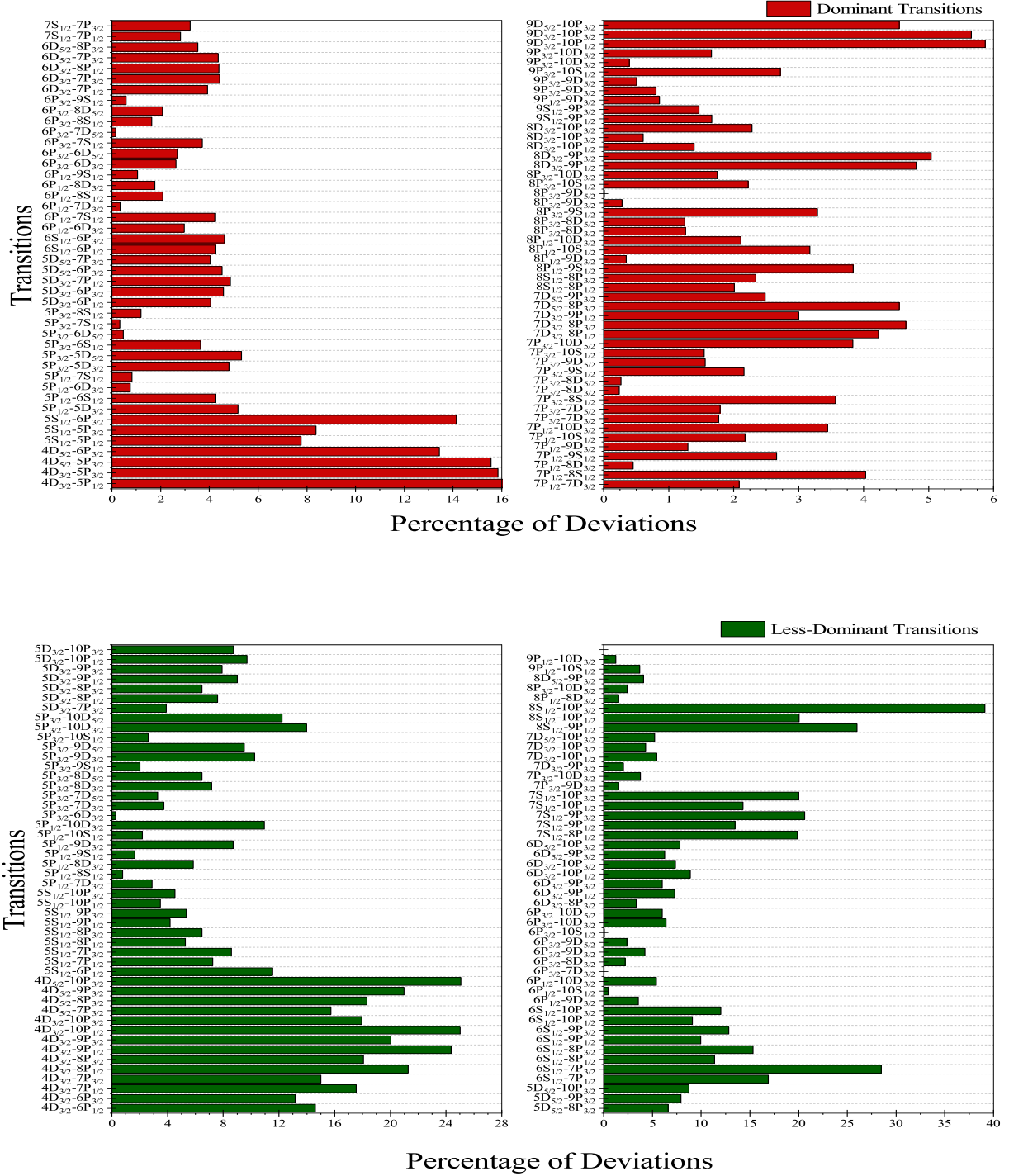


Figure 1. Percentage deviations of the oscillator strengths between the length (L) and velocity (V) gauge values of the E1 transitions in Zr IV. Dominant and less-dominant transitions are shown separately.

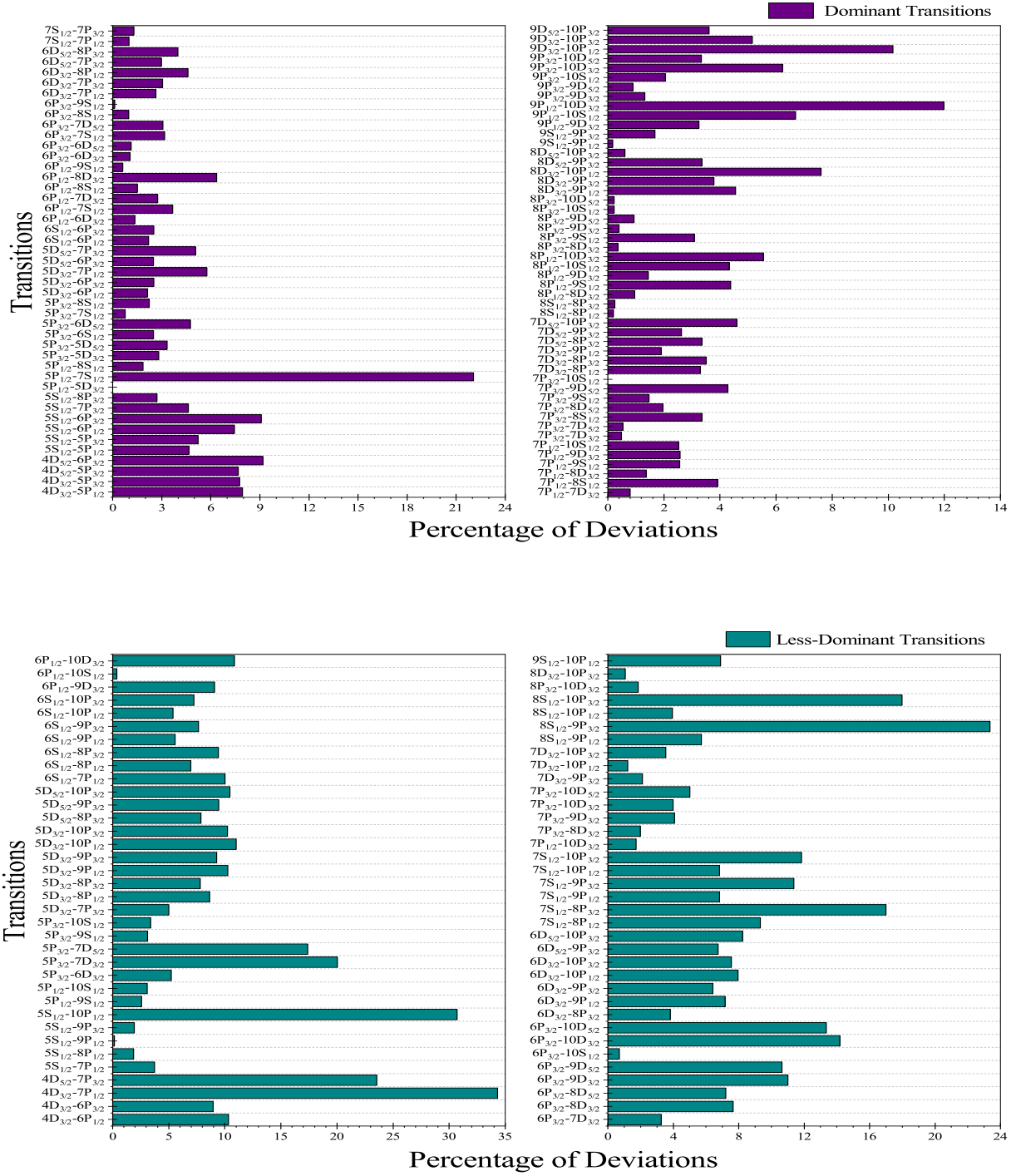


Figure 2. Percentage deviation of oscillator strengths between the L and V-gauge calculations in Nb V with dominantly and less dominantly contributing transitions shown separately.

3 RESULTS AND DISCUSSION

The detailed analysis of our results is given in this section along with the comparison of theoretical and experimental values available in the literature. First, we discuss the energies, line strengths, transition probabilities and oscillator strengths of all the transitions in both the ions. The uncertainties (quoted in the parentheses) for the S_{vk} , A_{vk} and f_{kv} values have been evaluated using the uncertainties in the E1 matrix elements, which are taken as the differences between the values from both the gauge expressions. We also depict percentage deviations of the oscillator strengths obtained using the V-gauge expression with respect to the L-gauge calculations for the important transitions of both the considered ions for better understanding of their differences. Then, the lifetimes of the low-lying states of these ions are estimated by using the above transition probabilities.

Our RMBPT calculated energy values for a few low-lying and excited states are given in Table 1 along with their comparison with the experimental values listed in NIST AD (Ralchenko et al. 2008). It is observed that the deviation of energy is maximum for the $4D_{3/2}$ state, viz., $\sim 11\%$ and 7% , respectively, in the Zr IV and Nb V ions. However, as we move on to less penetrating states, the deviation decreases rapidly up to $\sim 5\%$ and 3% for the $8S_{1/2}$ state in Zr IV and Nb V respectively, despite the slow convergence of perturbation expansion, thereby increasing the accuracy of our data. Besides, the energy values for the $7D$ states of Zr IV are not provided in the NIST AD. Therefore, the deviations of the energy values of these states could not be estimated.

We have listed our results for wavelengths λ , line strengths S_{vk} , transition probabilities A_{vk} and absorption oscillator strengths f_{kv} for Zr IV in Table 2. The λ values are estimated by using the experimental energies from the NIST AD (Ralchenko et al. 2008) wherever available. Otherwise, they are evaluated using our RMBPT method. Values from both the L and V gauge expressions are presented for the line strengths S_{vk} in the same table.

For the $9P_{3/2}-8S$ transition, we found that the reduced E1 matrix element is very small due to cancellation of large RPA contributions with the DF value. Correspondingly, the uncertainty in this particular transition is found to be very large to consider it reliable. Hence, we have not considered it for further spectroscopic analysis. During the investigation of data, it has been observed that the uncertainties in the A_{vk} and f_{kv} values are mostly small for many of the considered transitions except for the $4D_{3/2}-(6, 8, 9)P_{1/2}$, $4D_{3/2,5/2}-8P_{3/2}$, $5P_{3/2}-10D_{3/2}$, $6S_{1/2}-8P_{1/2}$, $7S_{1/2}-8P_{1/2,3/2}$, $(7, 8)S_{1/2}-9P_{3/2}$, $(7, 9)S_{1/2}-10P_{3/2}$ and $9S_{1/2}-10P_{1/2}$ transitions. The large errors in these transitions are the consequence of unusually large electron correlation effects exhibited by the high-lying states.

We have presented the percentage deviations of f_{kv} obtained using the two gauge expressions for different transitions in Fig. 1. It is seen from these plots that deviation varies from 0 to 8.5% for maximum number of dominantly contributing transitions, however a maximum deviation of 16% is seen for the $4D_{3/2}-5P_{1/2}$ transition. Oscillator strengths for less dominantly contributing transitions deviate majorly between $0-17\%$ and in the range $21-29\%$ for $4D_{3/2}-(9, 10)P_{3/2}$ and $6S_{1/2}-7P_{3/2}$ transitions. However, a maxima of $\sim 39\%$ is observed for the $8S_{1/2}-10P_{3/2}$ transition. It is also analyzed

that the $7S-8P_{3/2}$ transition shows an unreasonable percentage deviations of oscillator strengths for both the gauge expressions.

We have tabulated our results for Nb V in Table 3. The λ values are obtained by using energy values available in the NIST database for many of the transitions; otherwise they are estimated using our RMBPT calculations. Likewise Zr IV, the RPA and BO correlation contributions are found to be the dominant corrections towards the final values of dipole transition amplitudes. On account of our values of the calculated E1 matrix elements, we have evaluated S_{vk} values using both the L and V expressions and their uncertainties are estimated from the differences in these values. The A_{vk} and f_{kv} values along with the uncertainties are obtained using these line strengths. It has been observed from our calculations that the uncertainties in the values of transition probabilities and oscillator strengths are considerably small for maximum transitions except for the $4D_{3/2}-(7, 9, 10)P_{3/2}$, $4D_{3/2}-(8-10)P_{1/2}$, $4D_{5/2}-(9, 10)P_{3/2}$, $5S_{1/2}-10P_{3/2}$, $5P_{1/2,3/2}-(8-10)D_{3/2}$, $5P_{3/2}-(8-10)D_{5/2}$, $6S_{1/2}-7P_{3/2}$, $6P_{3/2}-10D_{5/2}$, $8P_{3/2}-8D_{5/2}$ and $9S_{1/2}-10P_{3/2}$ transitions. Among them, the results for the $4D_{3/2}-10P_{1/2}$, $5P_{1/2}-9D_{3/2}$ and $5P_{3/2}-9D_{5/2}$ transitions are found to be highly unreliable. Therefore, we have not provided further spectroscopic data for these three transitions specifically. We find that due to strong core-polarization effects arising through RPA causes such large uncertainties in the $4D_{3/2}-(7, 9, 10)P_{3/2}$, $4D_{3/2,5/2}-(8-10)P_{1/2}$, $4D_{5/2}-(9, 10)P_{3/2}$ and $5S_{1/2}-10P_{3/2}$ transitions.

We have presented plots for percent deviation of oscillator strengths of Nb V between the values obtained using both the gauge expressions and are shown in Fig. 2. In this figure, we separately present the values for dominantly and less dominantly contributing transitions. We observed that all the dominant transitions possess deviation less than 12% except for $5P_{1/2}-7S_{1/2}$ transition whose deviation lies at 22% . For the other transitions, deviations of less than 20% are observed for most of the transitions whereas a countable transitions have deviated from the L-gauge values in the range $23-35\%$. It is also perceived that the $4D_{3/2,5/2}-8P_{3/2}$, $5P_{1/2}-6S_{1/2}$ and $5P_{1/2}-(6, 7)D_{3/2}$ transitions show unusually large percentage deviations in the oscillator strengths.

We have also compared our results of the oscillator strengths and lifetimes of a few excited states of Zr IV with those are already available theoretical data in the literature for both the ions. Comparison of the oscillator strengths for the $4D_{3/2} \rightarrow 5P_{1/2,3/2}$, $4D_{5/2} \rightarrow 5P_{3/2}$ and $5S_{1/2} \rightarrow 5P_{1/2,3/2}$ transitions are made in Table 4. In this table, it is seen that the results for the transition probabilities and absorption oscillator strengths agree well with each other within the quoted error limits. We have found that our results are in perfect accord with the previous data published by Migdalek and Baylis (Migdalek & Baylis 1979) and are in fair agreement with the results reported by Migdalek in (Migdalek 2016) and Das et.al (Das et al. 2017) except for the $4D_{3/2} \rightarrow 5P_{1/2}$ and $4D_{5/2} \rightarrow 5P_{3/2}$ transitions. However, our results do not support the values obtained by Zilitis in (Zilitis 2007). This is so because, the results published in (Zilitis 2007) are obtained by employing the mean-field calculation at the DF level. We have seen in our calculations that the core-polarization as well as from other effects are contributing strongly to these transition properties, which were

Table 4. Comparison of the oscillator strengths for Zr IV and Nb V ions from our calculations with available theoretical data. Uncertainties are given in the parentheses.

Transition	Ion	f_{kv}			
		Present	(Migdalek & Baylis 1979)	(Zilitis 2007)	(Migdalek 2016) (Das et al. 2017)
$4D_{3/2} \rightarrow 5P_{1/2}$	Zr IV	0.127(20)		0.157	0.264
	Nb V	0.132(10)		0.161	0.266
$4D_{3/2} \rightarrow 5P_{3/2}$	Zr IV	0.0252(38)		0.0308	0.0260
	Nb V	0.0258(20)		0.0311	0.0258
$4D_{5/2} \rightarrow 5P_{3/2}$	Zr IV	0.154(23)			0.236
	Nb V	0.158(12)			0.235
$5S_{1/2} \rightarrow 5P_{1/2}$	Zr IV	0.312(24)	0.307	0.393	0.331
	Nb V	0.300(14)	0.297	0.385	0.326
$5S_{1/2} \rightarrow 5P_{3/2}$	Zr IV	0.660(54)	0.652	0.829	0.699
	Nb V	0.642(33)	0.638	0.821	0.697

Table 5. The estimated lifetimes τ (in ns) for a few excited states in Zr IV and Nb V ions and their comparisons with the available literature data. Uncertainties are given in the parentheses.

State	Zr IV	Nb V
$5P_{1/2}$	0.65(9)	0.29(2)
	0.588 (Zilitis 2007)	0.249 (Zilitis 2007)
	0.622 (Das et al. 2017)	0.274 (Das et al. 2017)
$5P_{3/2}$	0.61(8)	0.27(2)
	0.550 (Zilitis 2007)	0.238 (Zilitis 2007)
	0.5786 (Das et al. 2017)	0.259 (Das et al. 2017)
$5D_{3/2}$	0.54(1)	0.33(9)
$5D_{5/2}$	0.57(3)	0.35(1)
$6S_{1/2}$	0.51(1)	0.26(1)
$6P_{1/2}$	1.40(13)	0.54(4)
$6P_{3/2}$	1.50(16)	0.53(3)
$7S_{1/2}$	0.72(1)	0.35(1)
$7P_{1/2}$	2.46(23)	0.92(10)
$7P_{3/2}$	2.47(23)	0.92(9)
$8S_{1/2}$	0.66(1)	0.51(1)

neglected by Zilitis. This is why disparities between the results from both the works are seen.

Similarly, we have compared the absorption oscillator strengths of various transitions of Nb V in Table 4, according to which, our results are in good agreement with the results given by Das et.al. (Das et al. 2017). A deviation of less than 10% is seen during the comparison of our results with the data published in (Migdalek 2016), except for the $4D_{3/2} \rightarrow 5P_{1/2}$ and $4D_{5/2} \rightarrow 5P_{3/2}$ transitions. Our results show a variation of about 10 – 22% with respect to the theoretical data reported by Zilitis (Zilitis 2007) from the DF calculations.

The estimated lifetime values of the $5P_{1/2,3/2}$, $5D_{3/2,5/2}$, $6S_{1/2}$, $6P_{1/2,3/2}$, $7S_{1/2}$, $7P_{1/2,3/2}$ and $8S_{1/2}$ states of Zr IV have been listed in Table 5. Comparison of our calculated values for the $5P_{1/2,3/2}$ is also made in the same table. We notice that our results are in better agreement with the relativistic calculations presented by Das et.al. (Das et al. 2017) as compared to the values given by Zilitis (Zilitis 2007). The lifetimes for the $5P_{1/2,3/2}$, $5D_{3/2,5/2}$, $6S_{1/2}$, $6P_{1/2,3/2}$, $7S_{1/2}$, $7P_{1/2,3/2}$ and $8S_{1/2}$ states of Nb V are also given in Table 5. These values for the $5P_{1/2,3/2}$ states show reasonable agreement with available other theoretical data.

We believe that our aforementioned estimated values for various spectroscopic data are more reliable. Since the pre-

viously reported data do not quote the uncertainties in their calculations, our reported values will be useful in analysing various astrophysical processes involving the Zr IV and Nb V ions. Moreover, our precisely calculated values will be able to guide the future experiments and astrophysical observations to detect these spectroscopic properties.

4 CONCLUSION

By evaluating electric dipole matrix elements precisely, we have determined oscillator strengths, transition probabilities and lifetimes of many atomic states of the rubidium-isoelectronic zirconium and niobium ions. Calculations of the matrix elements were performed by accounting electron correlation effects through random-phase approximation, Brückner orbitals, structural radiation and normalization of wave functions over the mean-field values from the Dirac-Fock method. Our transition properties data include 192 transitions for Zr IV and 190 transitions for Nb V ion, while lifetimes are reported only for a few low-lying excited states in both the ions. We have also compared our results with the previously reported values for a few selected transition and find a reasonably good agreement among them except in

some cases. These data with the quoted uncertainties can be useful for many astrophysical applications and for their observations in the future.

ACKNOWLEDGEMENT

The work of B.A. is supported by SERB-TARE(TAR/2020/000189), New Delhi, India. The employed relativistic many-body method was developed in the group of Professor M. S. Safronova of the University of Delaware, USA.

DATA AVAILABILITY

The data underlying this article are available in the article.

REFERENCES

- Alonso-Medina A., Colón C., 2014, *Monthly Notices of the Royal Astronomical Society*, 445, 1567
- Blundell S., Guo D., Johnson W., Sapirstein J., 1987, *Atomic Data and Nuclear Data Tables*, 37, 103
- Chayer P., Fontaine M., Fontaine G., Wesemael F., Dupuis F., 2006, *Baltic Astronomy*, 15, 131
- Das A., Bhowmik A., Dutta N. N., Majumder S., 2017, *Journal of Physics B: Atomic, Molecular and Optical Physics*, 51, 025001
- García-Hernández D., García-Lario P., Plez B., Manchado A., d'Antona F., Lub J., Habing H., 2007, *Astronomy & Astrophysics*, 462, 711
- Glushkov A., Ambrosov S., Orlova V., Orlov S., Balan A., Serbov N., Dormostuchenko G., 1996, *Russian Physics Journal*, 39, 81
- Griem H., (Firm) E. S. . T., 1974, *Spectral Line Broadening by Plasmas*. Pure and applied physics a series of monographs and textbooks, Academic Press, <https://books.google.co.in/books?id=Nhp5AAAAIAAJ>
- Harper Jr C. L., 1996, *The Astrophysical Journal*, 466, 437
- Holden N. E., 1989, Technical report, Total half-lives for selected nuclides. National Nuclear Data Center, Upton, NY (USA)
- Iizuka T., Lai Y.-J., Akram W., Amelin Y., Schönbächler M., 2016, *Earth and Planetary Science Letters*, 439, 172
- Jeffery C., Behara N., Hibbert A., 2011, *Monthly Notices of the Royal Astronomical Society*, 412, 363
- Johnson W. R., 2007, *Atomic structure theory*. Springer
- Johnson W., Liu Z., Sapirstein J., 1996, *Atomic Data and Nuclear Data Tables*, 64, 279
- Karwowski J., Szulkin M., 1981, *Journal of Physics B: Atomic and Molecular Physics*, 14, 1915
- Kaur M., Dar D. F., Sahoo B., Arora B., 2020, *Atomic Data and Nuclear Data Tables*, p. 101381
- Kelleher D. E., Podobedova L., 2008, *Journal of Physical and Chemical Reference Data*, 37, 267
- Lindgård A., Nielsen S. E., 1977, *Atomic data and nuclear data tables*, 19, 533
- Martin I., Lavín C., Barrientos C., 1992, *International Journal of Quantum Chemistry*, 44, 465
- Migdalek J., 2016, *Journal of Physics B: Atomic, Molecular and Optical Physics*, 49, 185004
- Migdalek J., Baylis W., 1979, *Journal of Quantitative Spectroscopy and Radiative Transfer*, 22, 127
- Mohr P. J., Newell D. B., Taylor B. N., 2016, *J. Phys. Chem. Ref. Data*, 45, 043102
- Nahar S., 1995, *Astronomy and Astrophysics*, 293, 967
- Nilsson H., et al., 2010, *Astronomy & Astrophysics*, 511, A16
- Orban I., Glans P., Altun Z., Lindroth E., Källberg A., Schuch R., 2006, *Astronomy & Astrophysics*, 459, 291
- Palme H., Lodders K., Jones A., 2014, in Holland H. D., Turekian K. K., eds, , *Treatise on Geochemistry* (Second Edition), second edition edn, Elsevier, Oxford, pp 15–36, doi:<https://doi.org/10.1016/B978-0-08-095975-7.00118-2>, <https://www.sciencedirect.com/science/article/pii/B9780080959757001182>
- Qin Z., Zhao J., Liu L., 2019, *Journal of Quantitative Spectroscopy and Radiative Transfer*, 227, 47
- Ralchenko Y., Kramida A., Reader J., et al., 2008, National Institute of Standards and Technology, Gaithersburg, MD
- Rauch T., Quinet P., Hoyer D., Werner K., Demleitner M., Kruk J., 2016, *Astronomy & Astrophysics*, 587, A39
- Rauch T., Gamrath S., Quinet P., Löbbling L., Hoyer D., Werner K., Demleitner M., 2017, *Astronomy & Astrophysics*, 599, A142
- Ruffoni M., Den Hartog E., Lawler J., Brewer N., Lind K., Nave G., Pickering J., 2014, *Monthly Notices of the Royal Astronomical Society*, 441, 3127
- Safronova U., Safronova M., Johnson W., 2005, *Physical Review A*, 71, 052506
- Sen K., Puri A., 1989, *Physics Letters A*, 137, 128
- Sobelman I. I., 1979, in , *Atomic Spectra and Radiative Transitions*. Springer, pp 53–88
- Tayal S., 2012, *Astronomy & Astrophysics*, 541, A61
- Vanture A. D., Wallerstein G., Brown J. A., 1994, *Publications of the Astronomical Society of the Pacific*, 106, 835
- Wittkowski M., 2005, *Bulletin de la Société Royale des Sciences de Liège*, 74, 165
- Začs L., Barzdis A., Sandars M., Matrozi E., 2011, in *Niobium in the spectra of metal-poor stars*. p. 287, doi:[10.22323/1.100.0287](https://doi.org/10.22323/1.100.0287)
- Zeippen C., 1995, *Physica Scripta*, 1995, 43
- Zilitis V., 2007, *Optics and Spectroscopy*, 103, 895
- Zilitis V., 2009, *Optics and Spectroscopy*, 107, 54

This paper has been typeset from a \LaTeX file prepared by the author.